Thin-Sheet Dynamics of Subduction

Neil M. Ribe
Laboratoire FAST, Orsay (France)

In collaboration with:

Eléonore Stutzmann (IPG Paris)

Zhonghai Li (Chinese Academy of Geological Sciences)

Bingrui Xu (Fudan Univ.)

Gianluca Gerardi (FAST)

Paul Tackley (ETH)

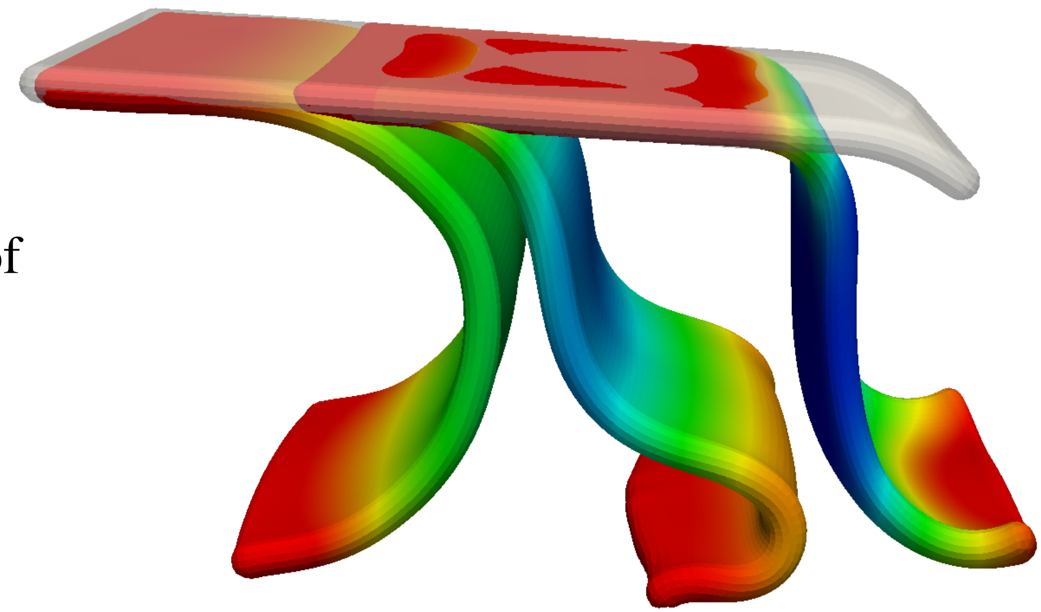

The Lithosphere as a Thin Sheet

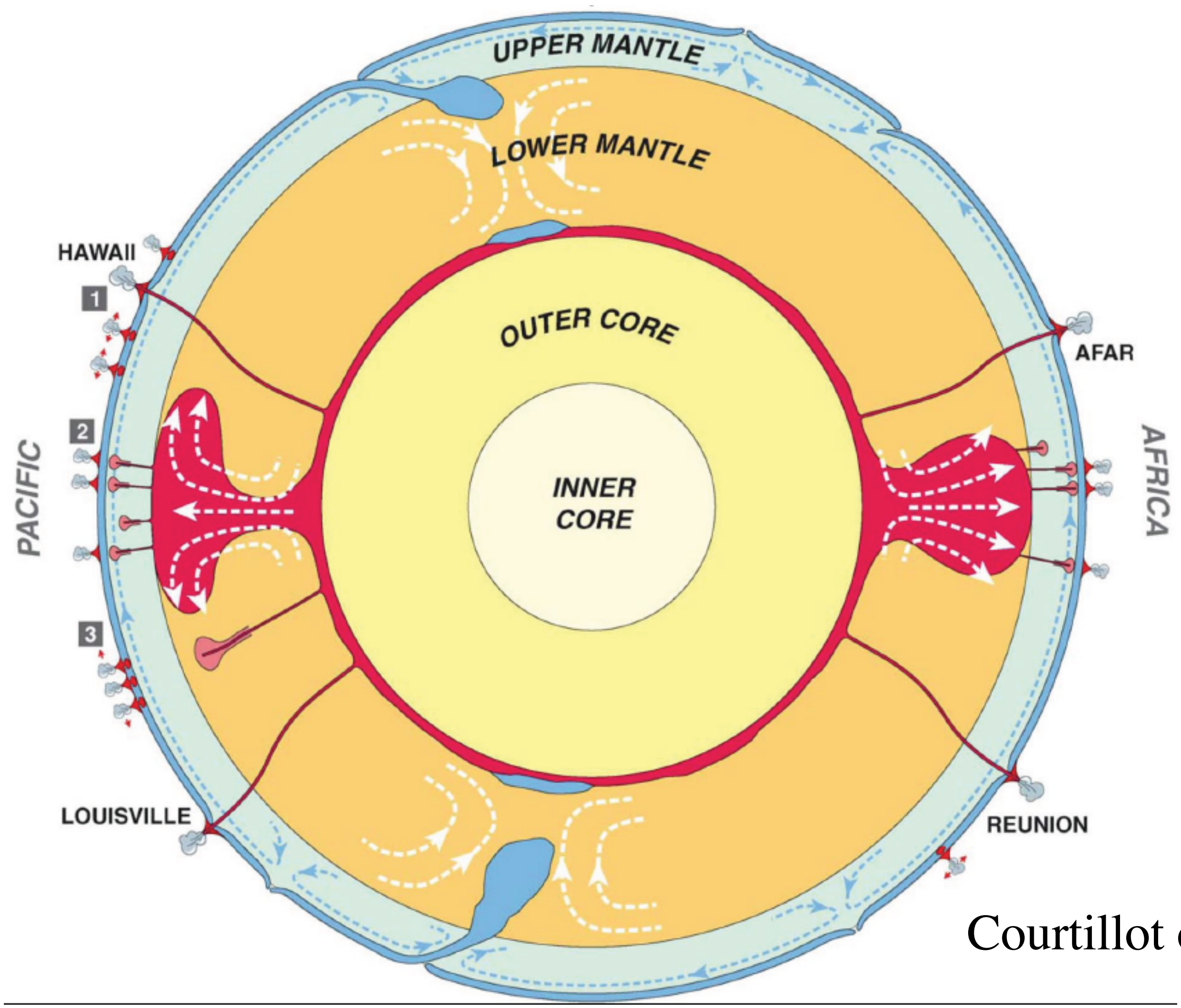

Courtillot et al. (2003)

The Lithosphere as a Thin Sheet

Subduction →

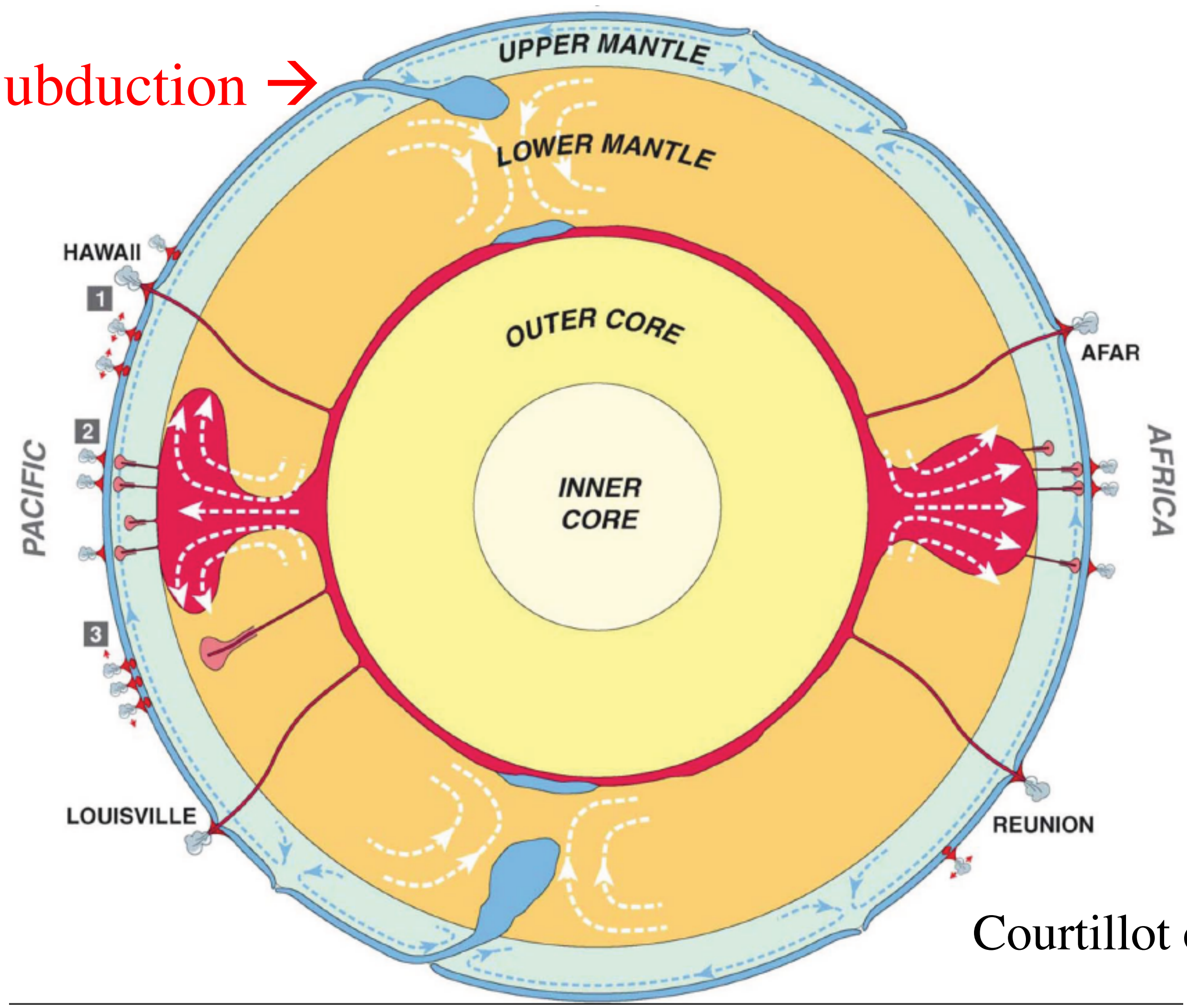

Courtillot et al. (2003)

Theory of Thin Viscous Sheets

Deformation of Thin Sheets: Stretching vs. Bending

Dominant stress component: layer-parallel normal stress σ_{ss}

Stretching:

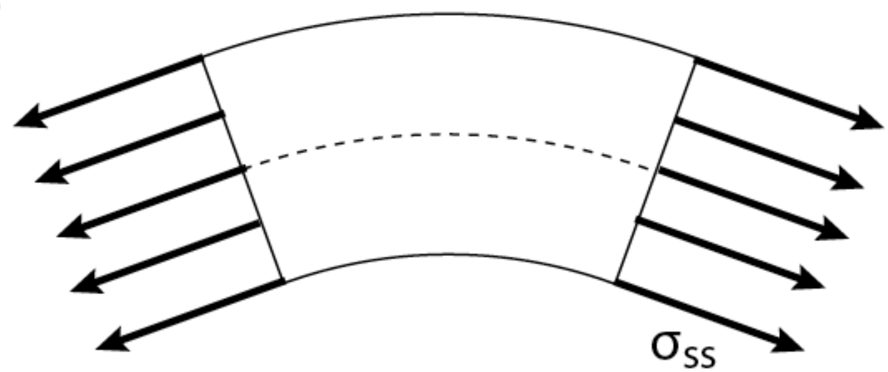

Bending:

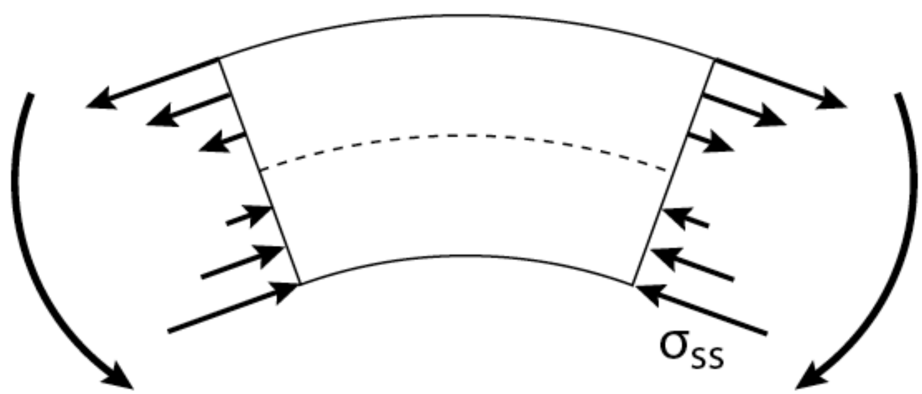

Thin-sheet theory: Essential concepts (in 2-D)

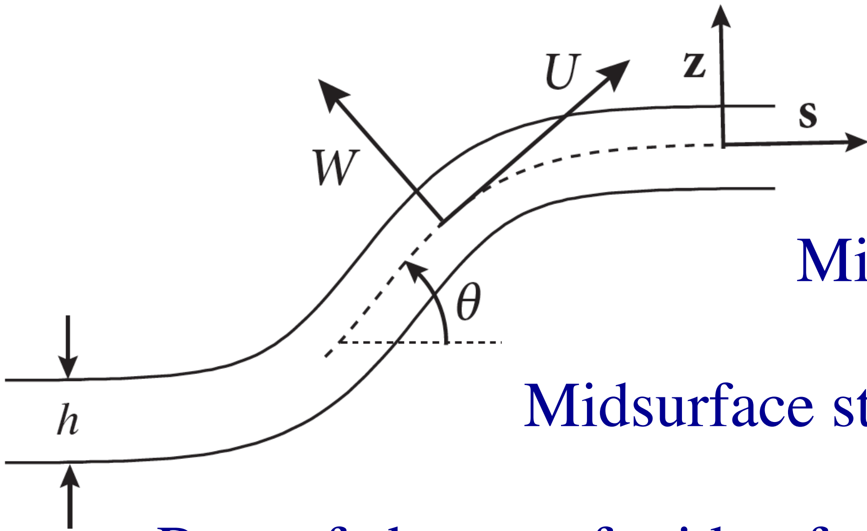

Midsurface curvature: $K = \partial_s \theta$

Midsurface velocity: $\mathbf{U} = U\mathbf{s} + W\mathbf{z}$

Midsurface stretching rate: $\Delta = \partial_s U - KW$

Rate of change of midsurface curvature: $\dot{K} = \partial_s(\partial_s W + KU)$

Fiber stress resultant: $$N = \int_{-h/2}^{h/2} \sigma_{ss} \mathrm{d}z$$

Shear stress resultant: $$Q = \int_{-h/2}^{h/2} \sigma_{sz} \mathrm{d}z$$

Bending moment: $$M = \int_{-h/2}^{h/2} z\sigma_{ss} \mathrm{d}z$$

Complete Set of Equations for a Deforming Viscous Sheet

Force balance: $N' - KQ = -hg_s\delta\rho, \quad Q' + KN = -hg_z\delta\rho$

Torque balance: $M' = Q$

Stress resultant: $N = 4\eta h\Delta$

Bending moment: $M = -\dfrac{\eta h^3}{3}\dot{K}$

Evolution of the midsurface shape: $\dfrac{\mathrm{D}\mathbf{x}}{\mathrm{D}t} = U\mathbf{s} + W\mathbf{z}$

Evolution of the thickness: $\dfrac{\mathrm{D}h}{\mathrm{D}t} = -\Delta h$

3-D Boundary-Element Modeling of Subduction

Morphologies of Subducted Slabs

Terrestrial subduction zones
(Schellart 2010)

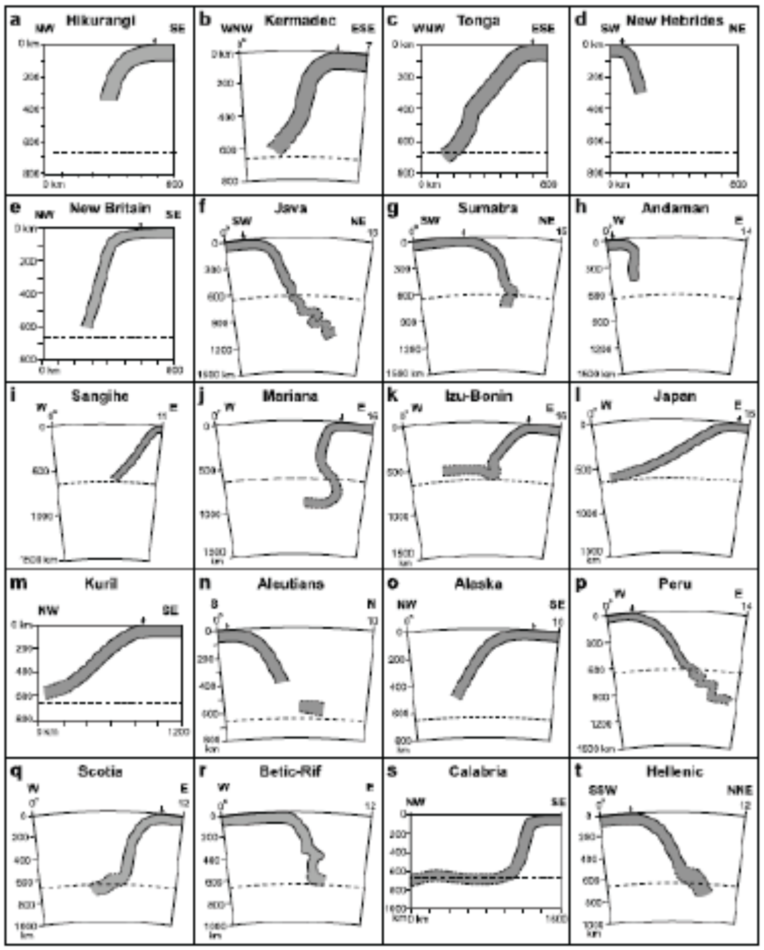

Laboratory experiments
(Roma-TRE group)

viscosity contrast

dripping

$\gamma = 3.6$

weak retreating

3600

folding
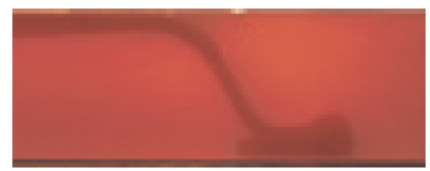
3600

advancing
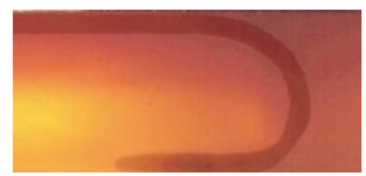
3600

strong retreating

350000

3-D Model Problem

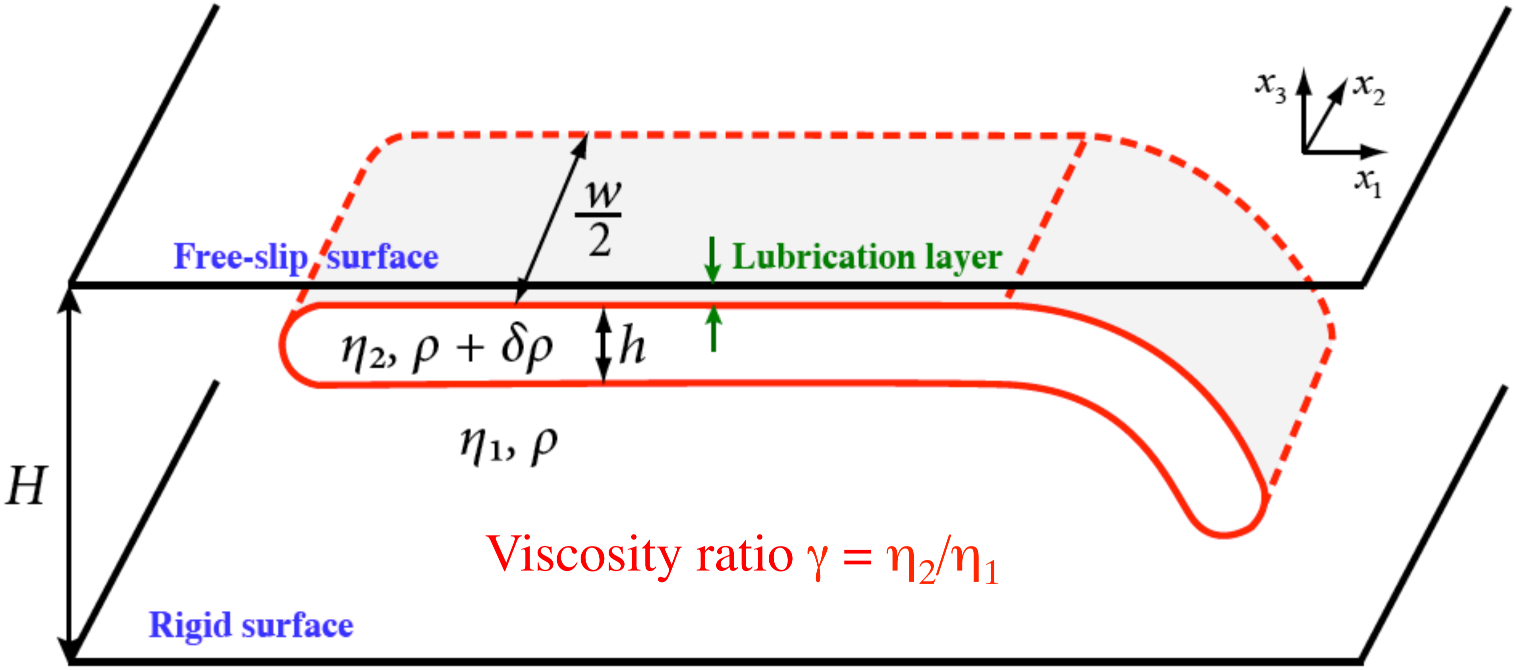

- Viscous sheet immersed in a fluid layer with much lower viscosity
- Free-slip upper surface, rigid lower surface
- Thin lubrication layer between upper surface and sheet
- Subduction initiated by bending down one edge of the sheet

Boundary-Element Method

Velocity at a point x_0 on the interface satisfies the integral equation

$$\frac{1+\gamma}{2}\mathbf{u}(\mathbf{x}_0) = -\frac{\delta\rho}{\eta_1}\int_S (\mathbf{g}\cdot\mathbf{x})\underbrace{\mathbf{n}(\mathbf{x})}_{\text{unit normal}}\cdot\underbrace{\mathbf{J}(\mathbf{x}-\mathbf{x}_0)}_{\text{Velocity Green function}}\mathrm{d}S(\mathbf{x})$$

Buoyancy integral

$$+(1-\gamma)\int_S \mathbf{u}(\mathbf{x})\cdot\underbrace{\mathbf{K}(\mathbf{x}-\mathbf{x}_0)}_{\text{Stress Green function}}\cdot\mathbf{n}(\mathbf{x})\mathrm{d}S(\mathbf{x})$$

Interfacial velocity integral

Advantages:

- Reduction of dimensionality (3D → 2D)
- No sidewall effects
- Green functions can be designed to satisfy top + bottom boundary conditions automatically

Unsteady Subduction

$(\eta_2/\eta_1 = 200)$

Initial configuration:

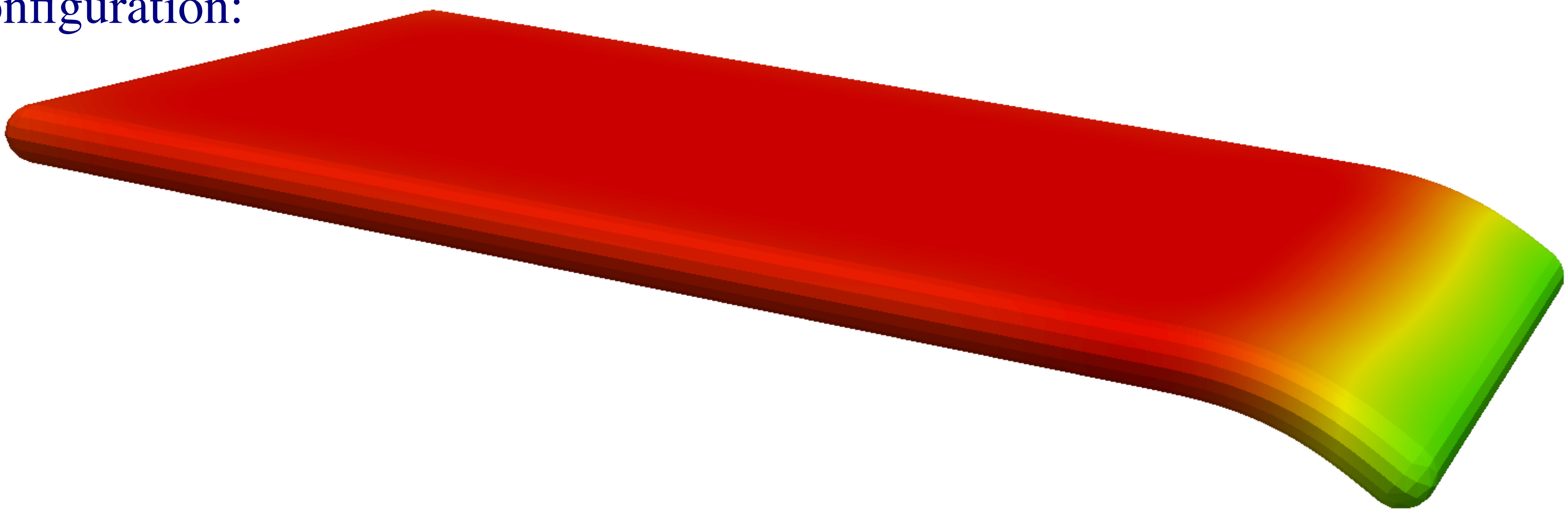

Unsteady Subduction

$(\eta_2/\eta_1 = 200)$

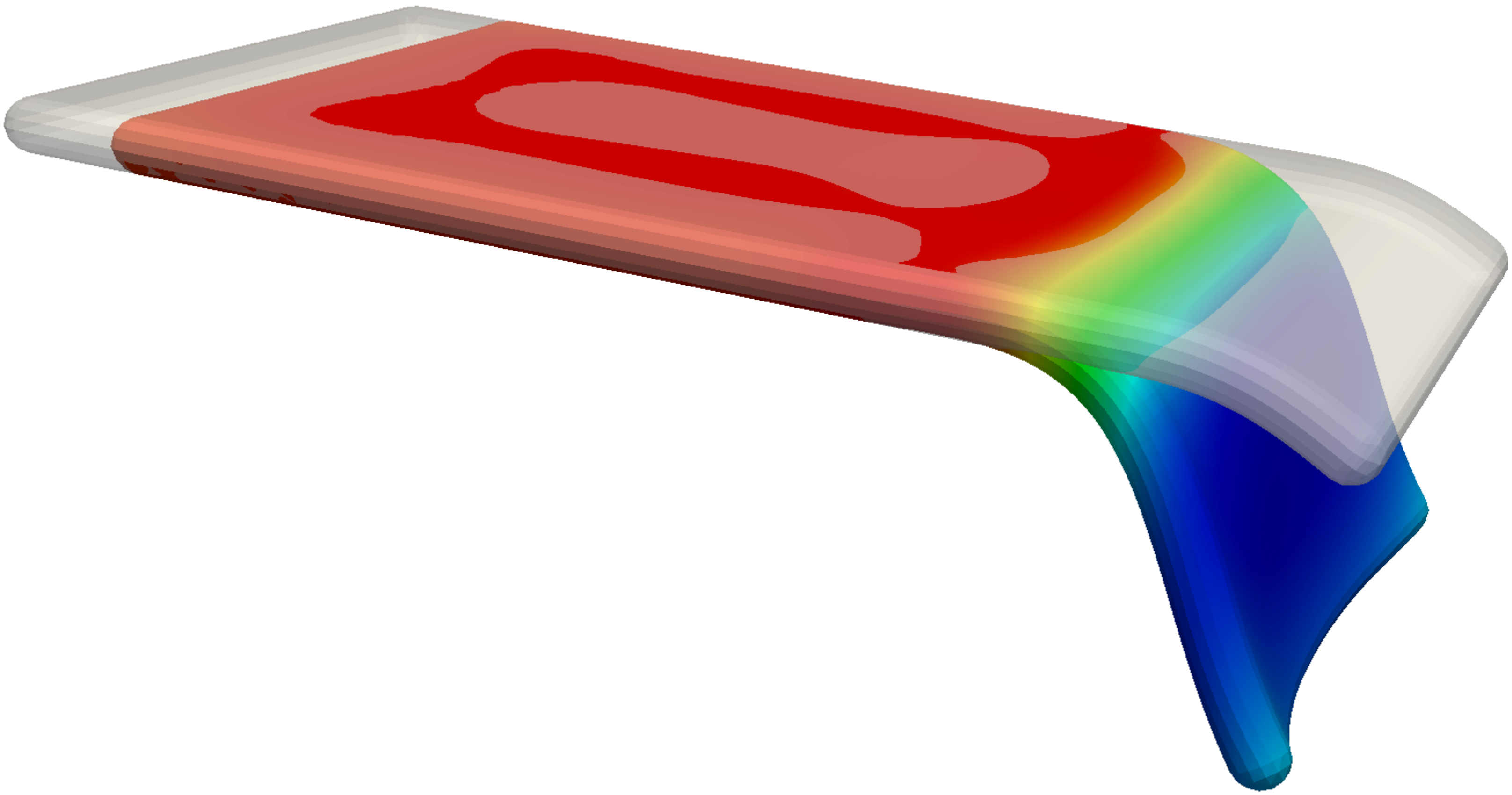

Unsteady Subduction

$(\eta_2/\eta_1 = 200)$

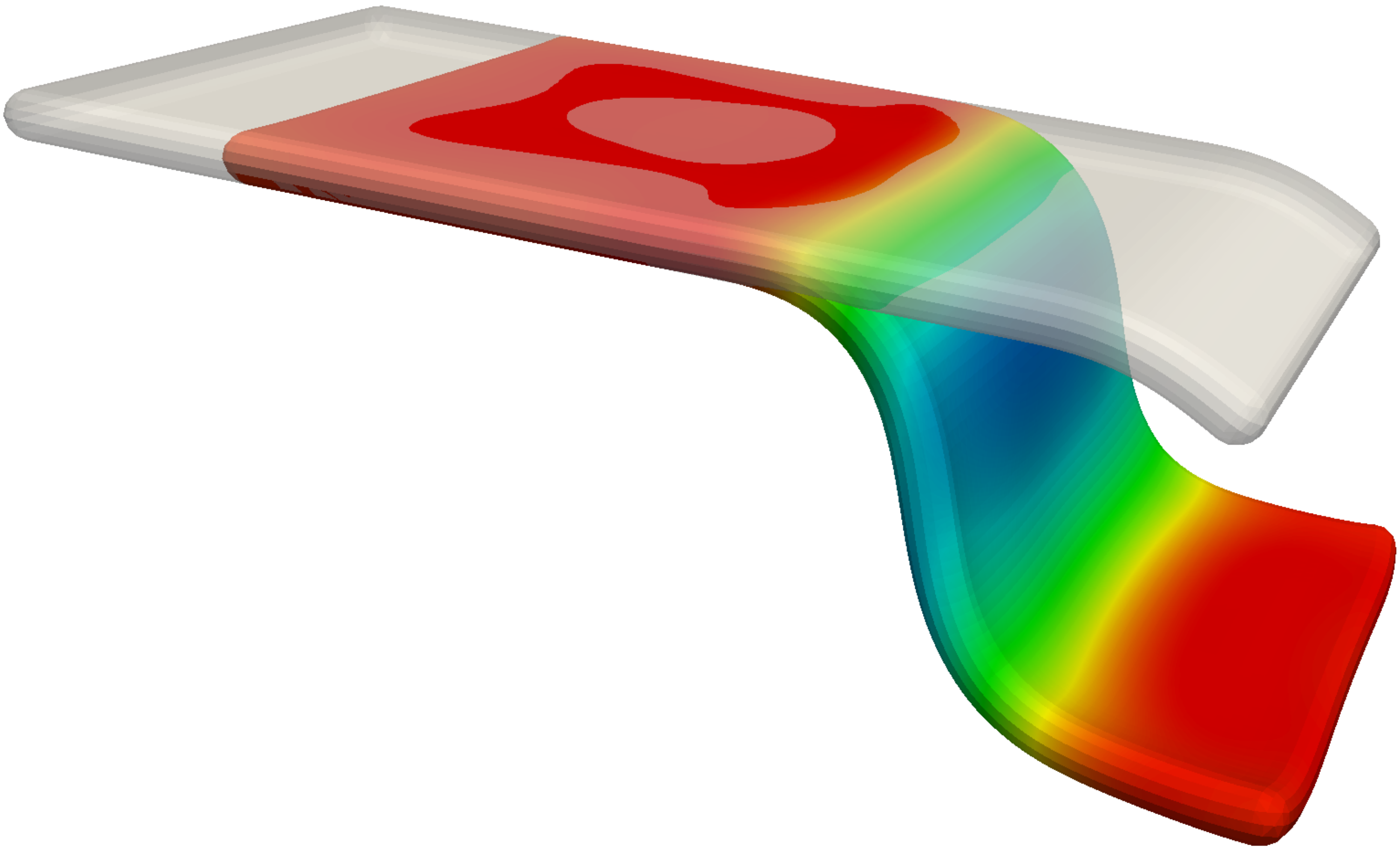

Unsteady Subduction

$(\eta_2/\eta_1 = 200)$

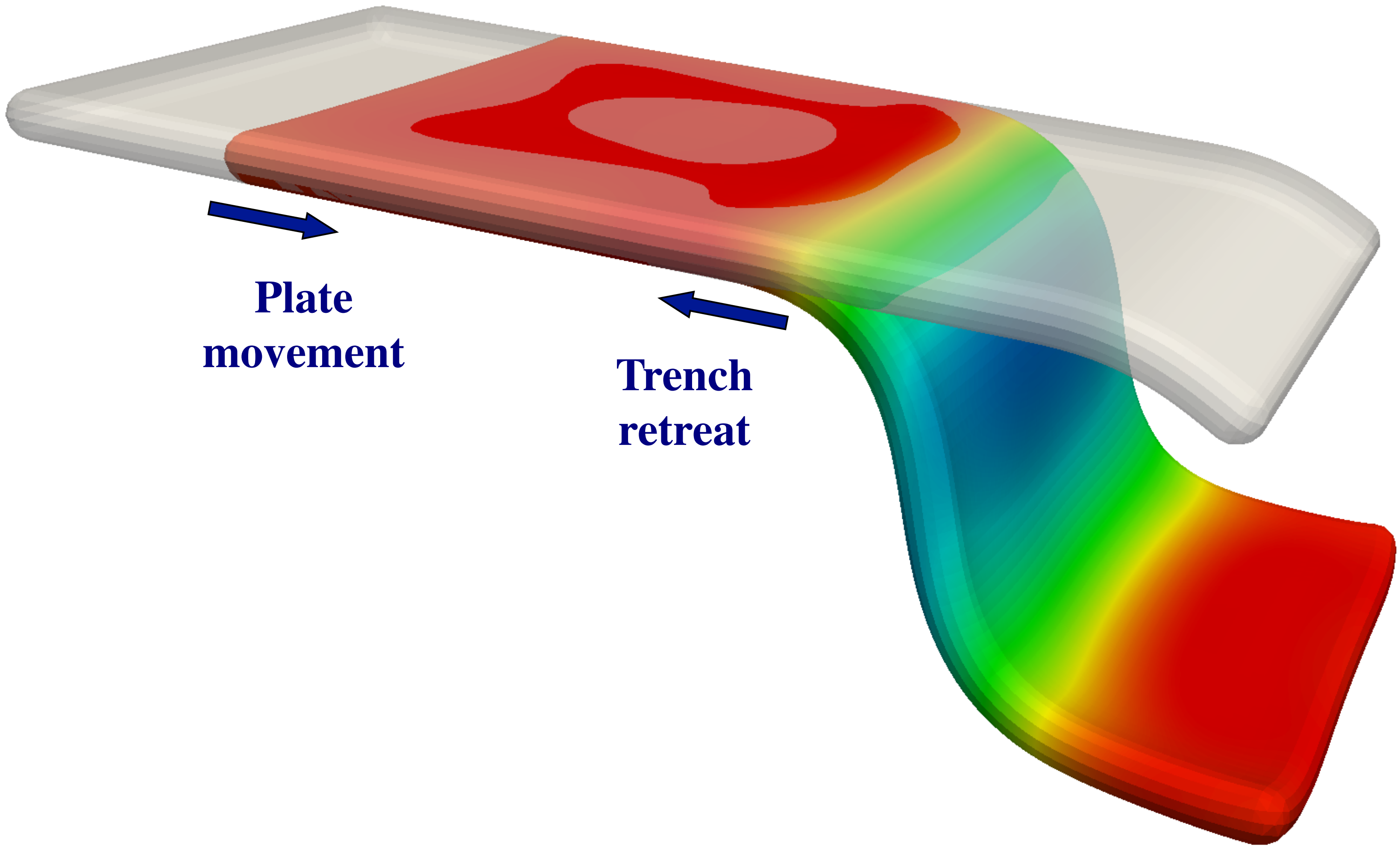

Bending Length

Definition: l_b = length of the sheet's midsurface where deformation by bending is concentrated (= slab + flexural bulge)

Calculation:

- Assume infinitely deep layer ($H \to \infty$)
- Instantaneous BEM solution for the geometry shown
- Use thin-sheet theory to calculate M

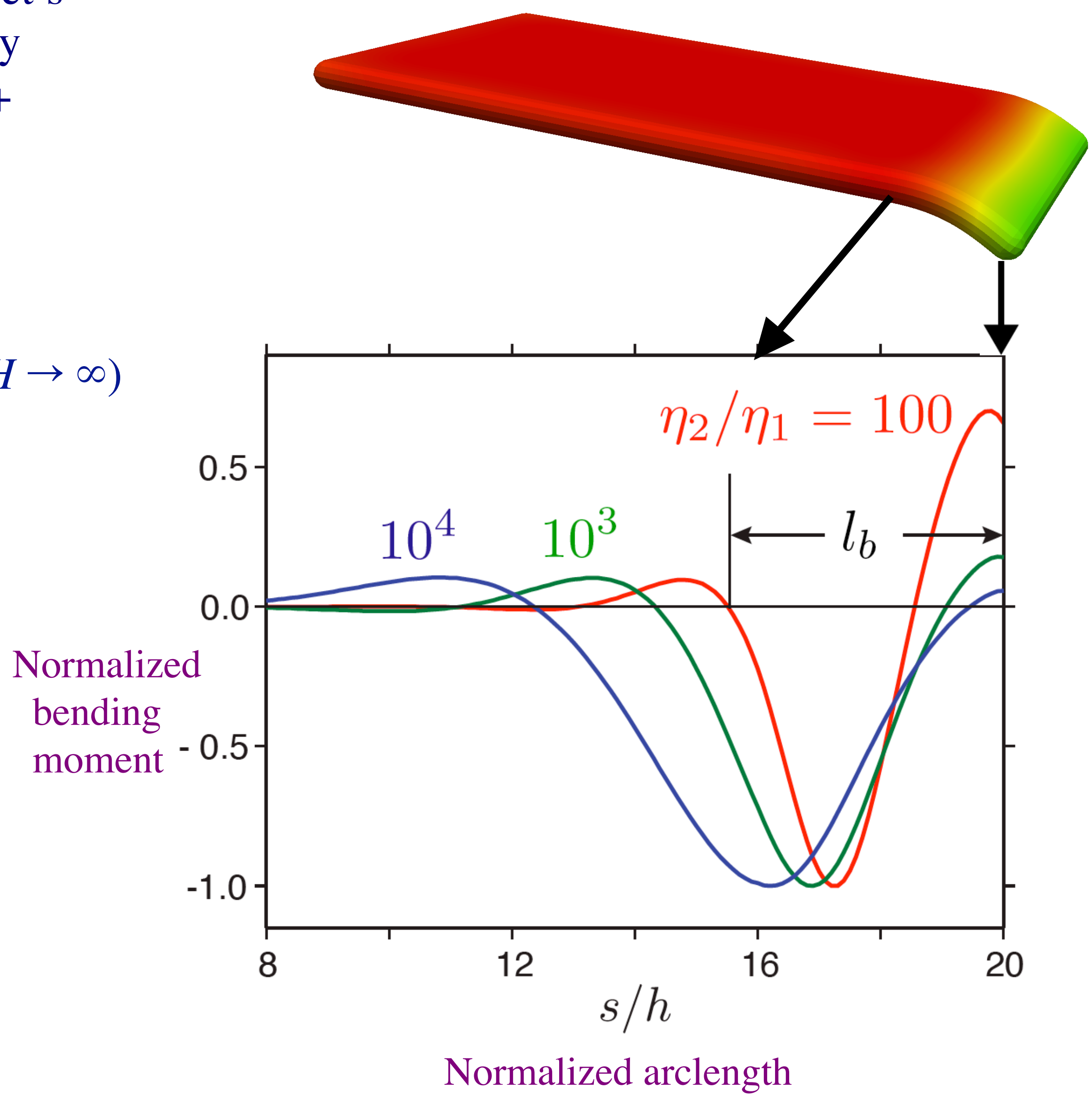

Bending Length

Definition: l_b = length of the sheet's midsurface where deformation by bending is concentrated (= slab + flexural bulge)

Calculation:

- Assume infinitely deep layer ($H \rightarrow \infty$)
- Instantaneous BEM solution for the geometry shown
- Use thin-sheet theory to calculate M

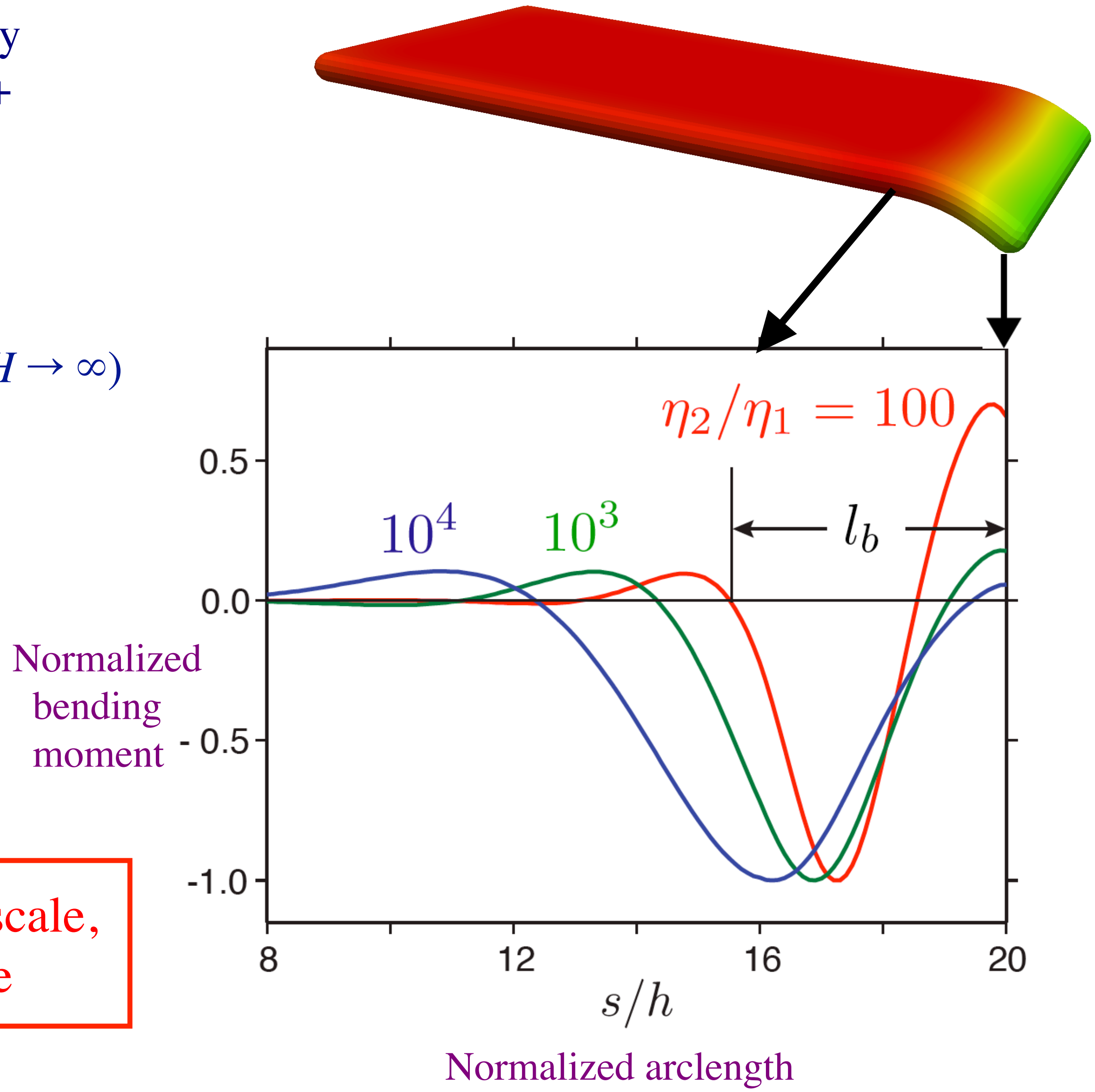

l_b is a *dynamic* length scale, not a geometric one

Scaling Analysis of Free Subduction

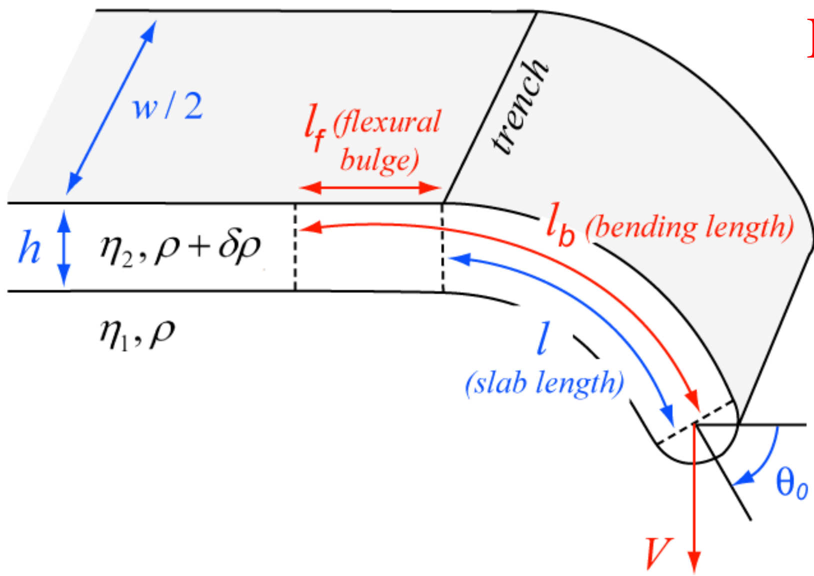

Forces on the bending portion of the sheet:

external drag: $F_{\text{ext}} \sim \eta_1 V w$

internal bending resistance: $F_{\text{int}} \sim \eta_2 h^3 V w / l_b^3$

buoyancy: $F_{\text{buoy}} \sim h l w g \delta\rho$

balance buoyancy and external drag:

$$F_{\text{buoy}} \sim F_{\text{ext}} \rightarrow V \sim \frac{h l g \delta\rho}{\eta_1} \equiv V_{\text{Stokes}}$$

ratio of internal to external viscous forces:

$$\boxed{\frac{F_{\text{int}}}{F_{\text{ext}}} \sim \frac{\eta_2}{\eta_1}\left(\frac{h}{l_b}\right)^3 \equiv S}$$

Flexural stiffness

Universal Scaling of the Sinking Speed

- 109 instantaneous BEM solutions for different values of l/h, w/l, and η_2/η_1
- constant dip angle θ_0 (= 60°) to ensure geometrical similarity of midsurface shape

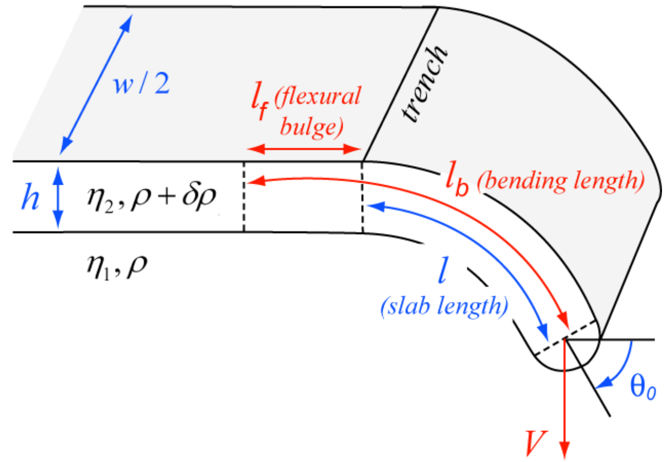

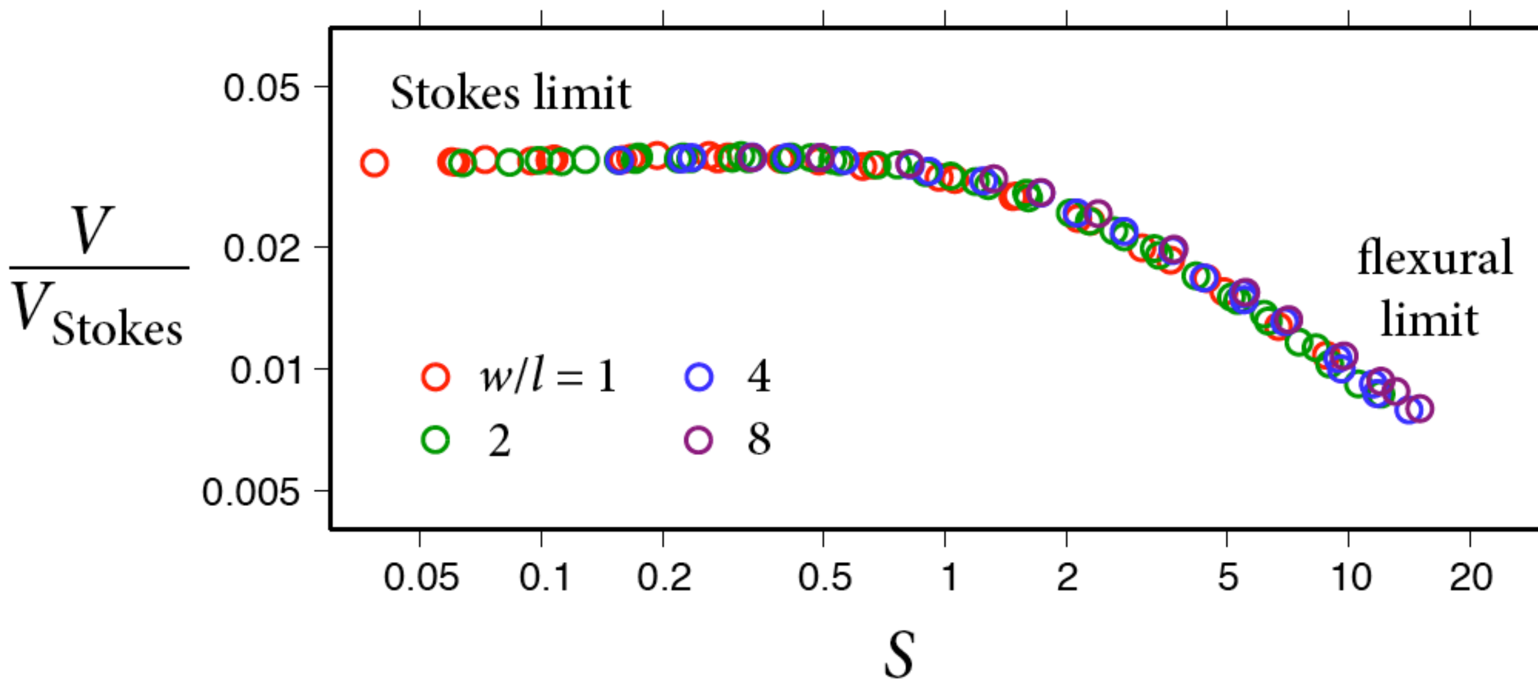

Subduction Modes: Regime Diagram

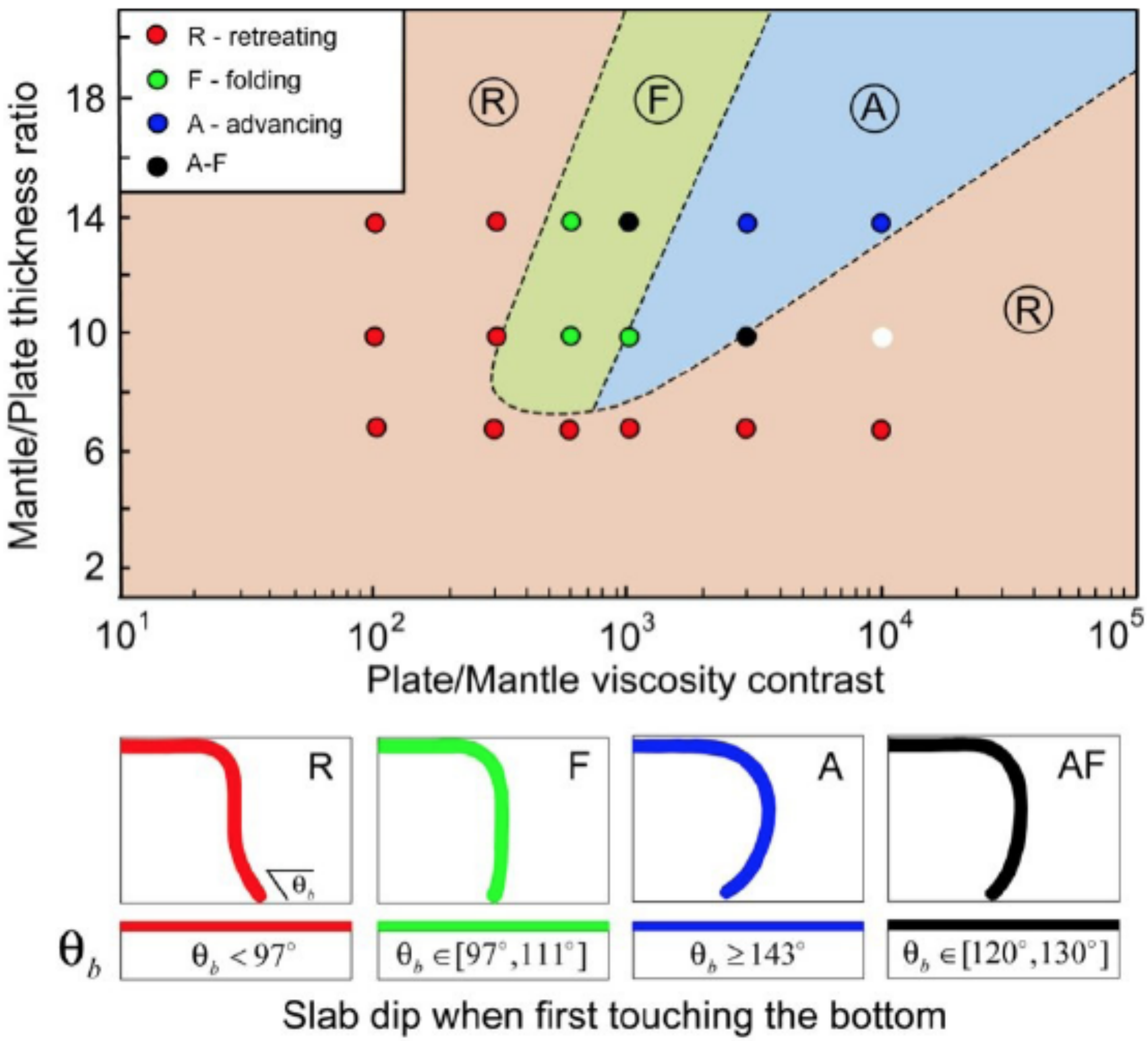

Circles: 3-D BEM predictions

Background colors: experimental regime diagram (Schellart 2008)

Mode selection controlled by slab incidence angle on bottom boundary

Periodic Folding of Viscous Sheets

Periodic Folding of a Viscous Sheet

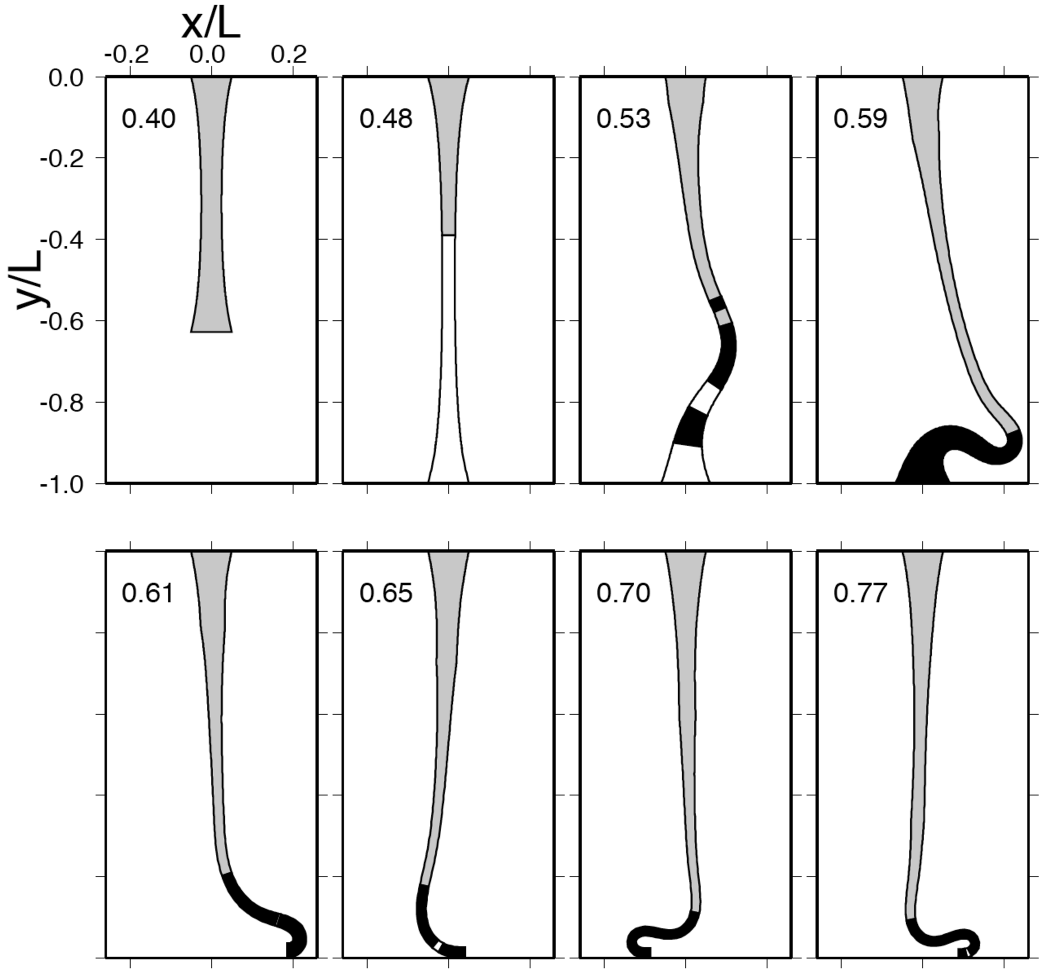

grey = extension
white = compression
black = bending

Two Modes of Periodic Folding

Parameter definitions

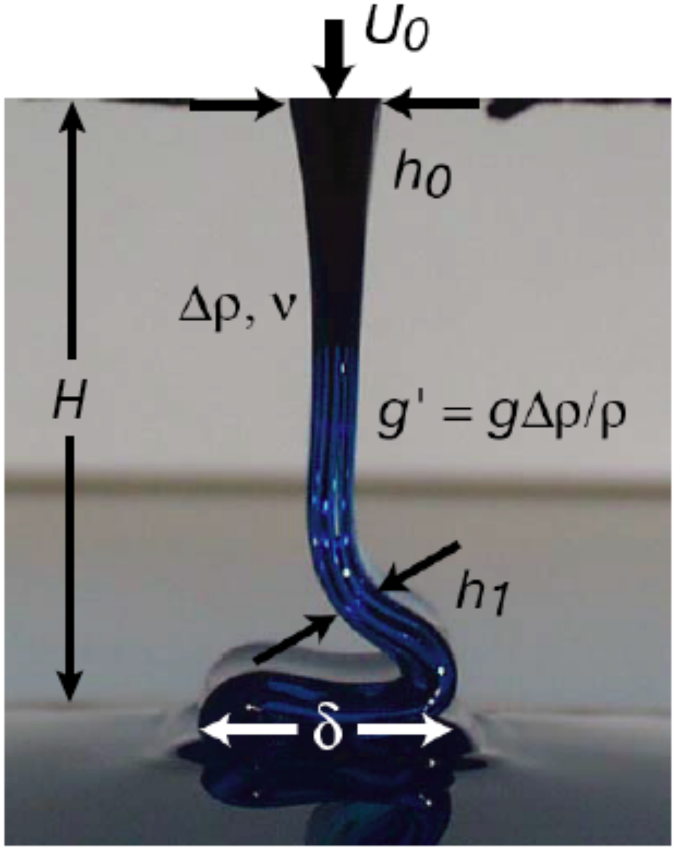

Regime diagram

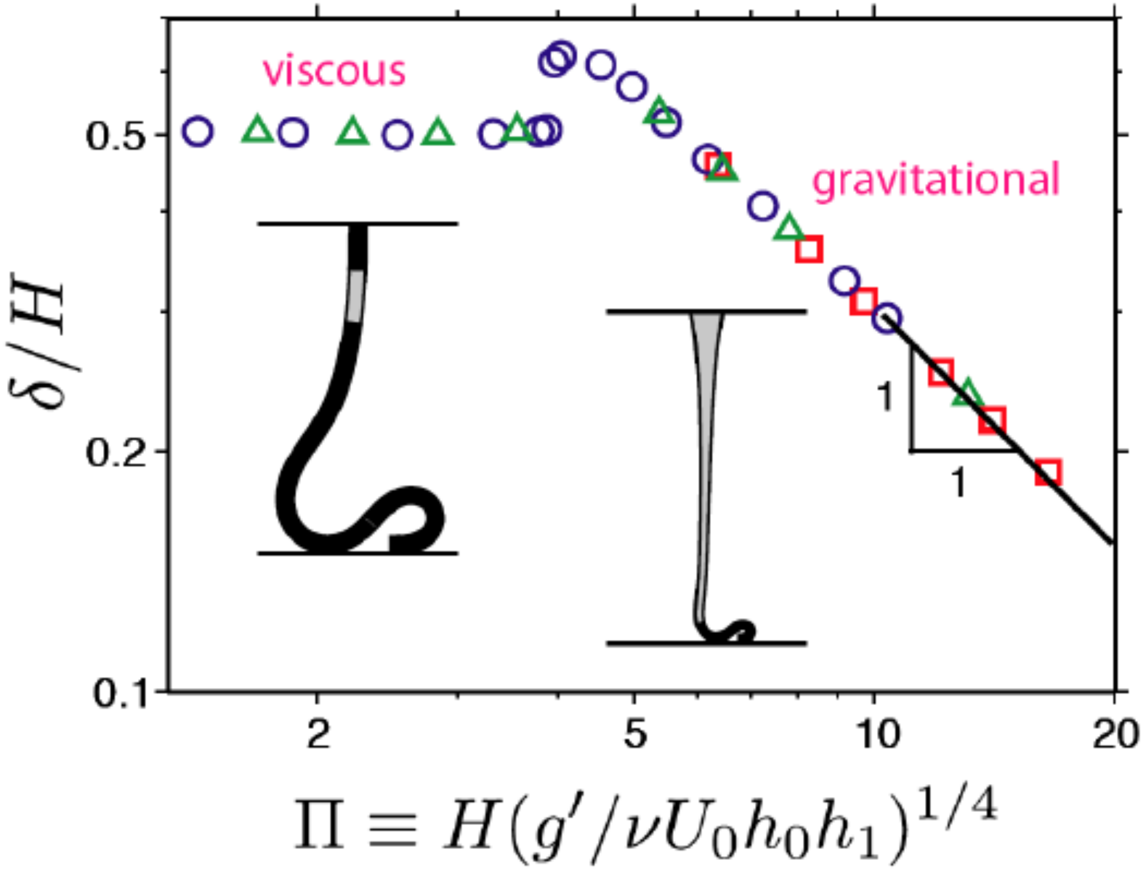

Comparison with laboratory experiments

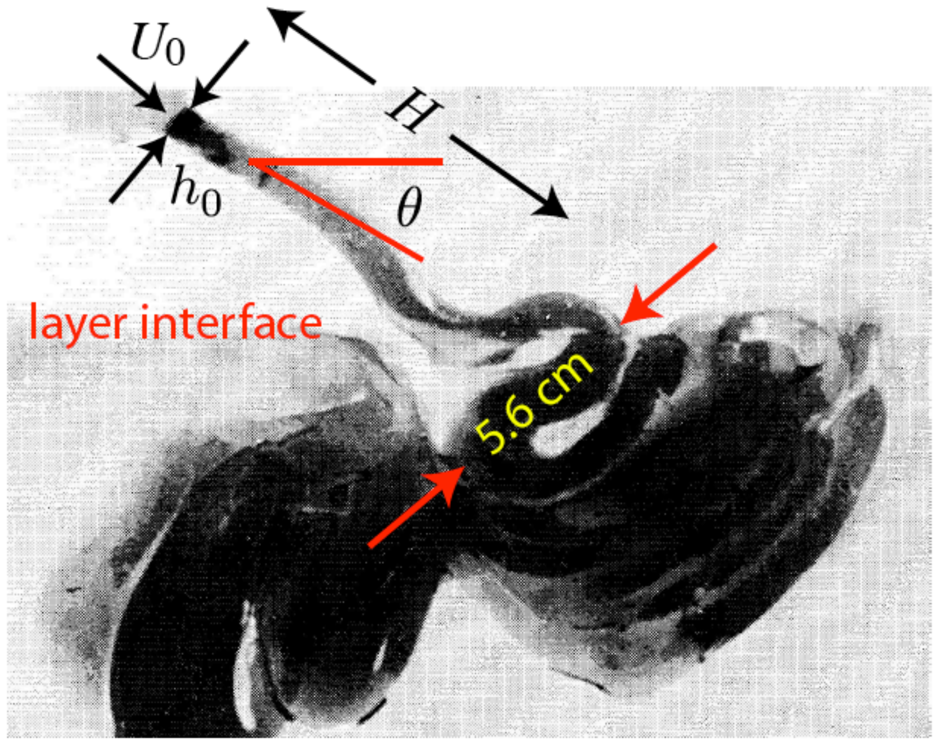

Image from Guillou-Frottier et al. (1995)

prediction of the scaling law:

$\Delta\rho$ (kg m^{-3})	μ (Pa s)	h_0 (cm)	U_0 (cm s^{-1})	θ (deg)	H (cm)	B	Π	δ (cm)
58	7×10^5	1.0	0.05	35	9.3	0.008	0.91	5.7

→ **agrees within 2%**

Periodic slab folding beneath central America?

Scaling law predicts $\delta \sim 460$ km

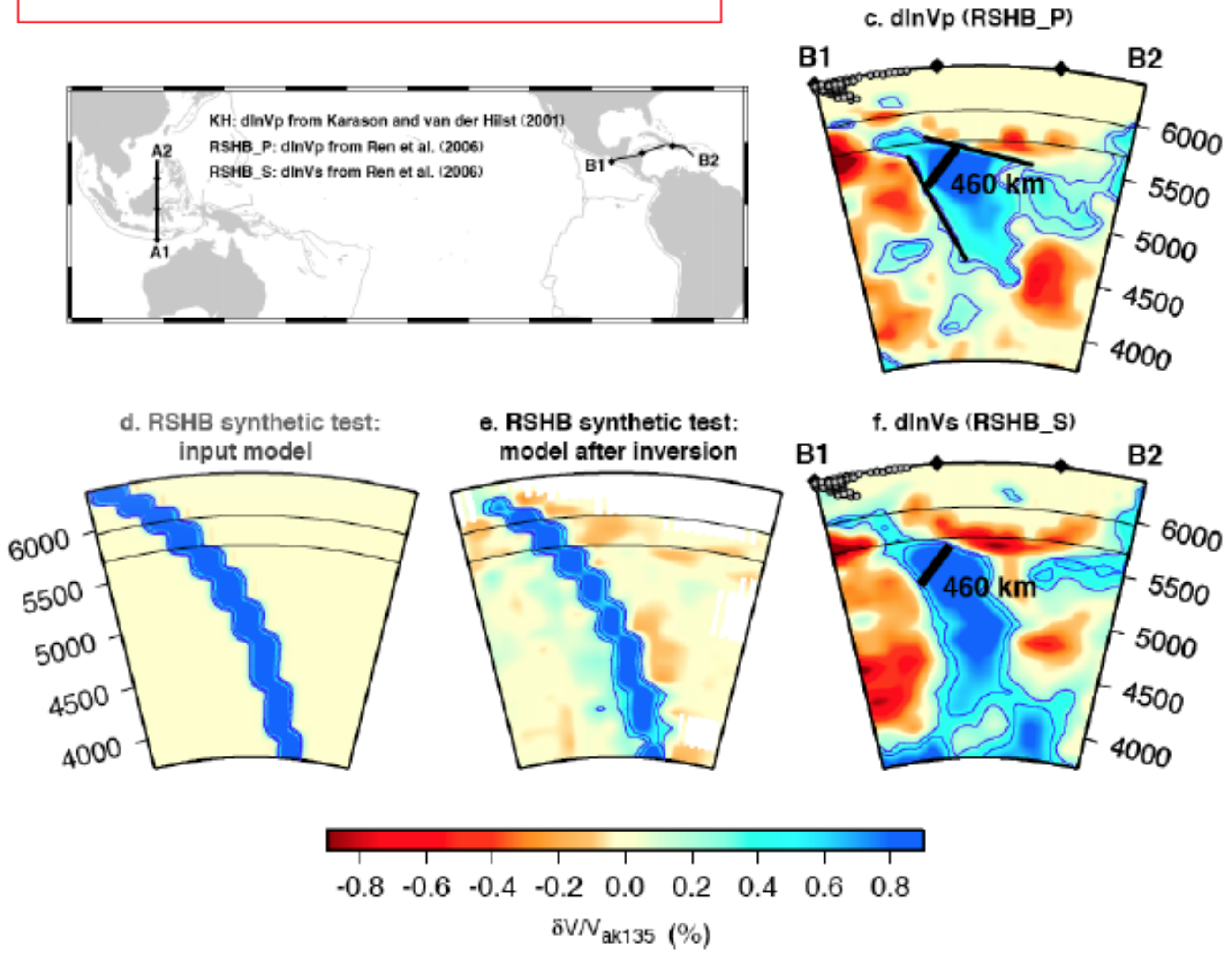

Periodic Slab Folding in Numerical Models

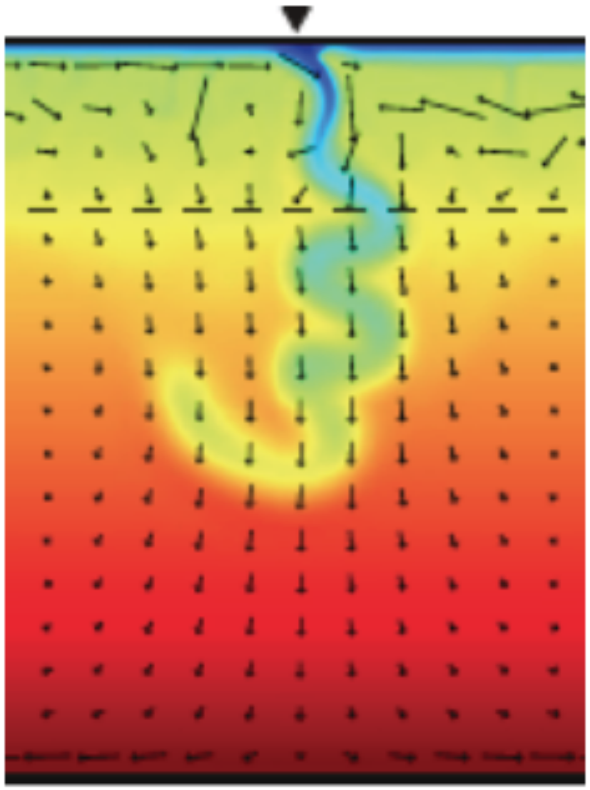

Lee and King (2011)

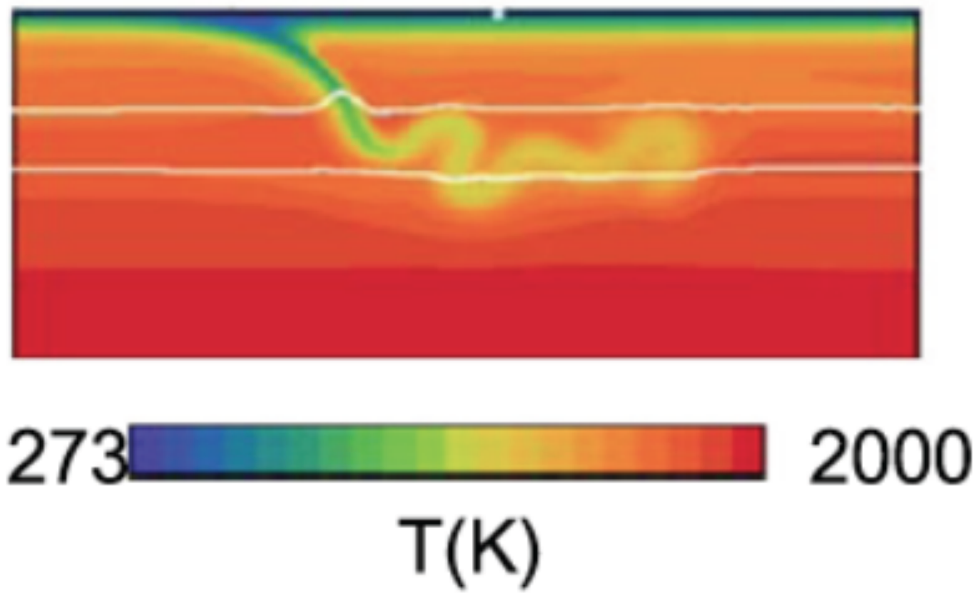

Cizkova and Bina (2013)

Combining the Boundary-Integral Representation with Thin-Sheet Theory

Hybrid Boundary-Integral / Thin-Sheet (BITS) model

(Xu & Ribe 2016)

Goal: a boundary-integral model that incorporates thin-sheet theory directly

Starting point: full 2-D boundary-integral representation for both fluids

Massage gently to obtain a single integral equation for the midsurface velocity:

$$\mathbf{U}(s) = \frac{1}{\eta_2}\int_0^L \underbrace{[\gamma \mathbf{g} h(p)\delta\rho}_{\text{buoyancy}} + \underbrace{(\gamma - 1)\mathbf{N}'(p)]}_{\text{viscous forces}} \cdot \underbrace{\mathbf{J}(\mathbf{x}_0(p) - \mathbf{x}_0(s))}_{\text{velocity Green's function}}\mathrm{d}p$$

Force vector: $$\mathbf{N} = \underbrace{4\eta_2 h(\mathbf{U}' \cdot \mathbf{s})\mathbf{s}}_{\text{stretching}} + \underbrace{\frac{\eta_2}{3}[h^3(\mathbf{U}' \cdot \mathbf{z})']'\mathbf{z}}_{\text{bending}}$$

Evolution equations: $$\frac{\mathrm{D}\mathbf{x}_0}{\mathrm{D}t} = \mathbf{U}, \qquad \frac{\mathrm{D}h}{\mathrm{D}t} = -h\mathbf{U}' \cdot \mathbf{s}$$

BITS Model: Evolution of the Sheet's Shape

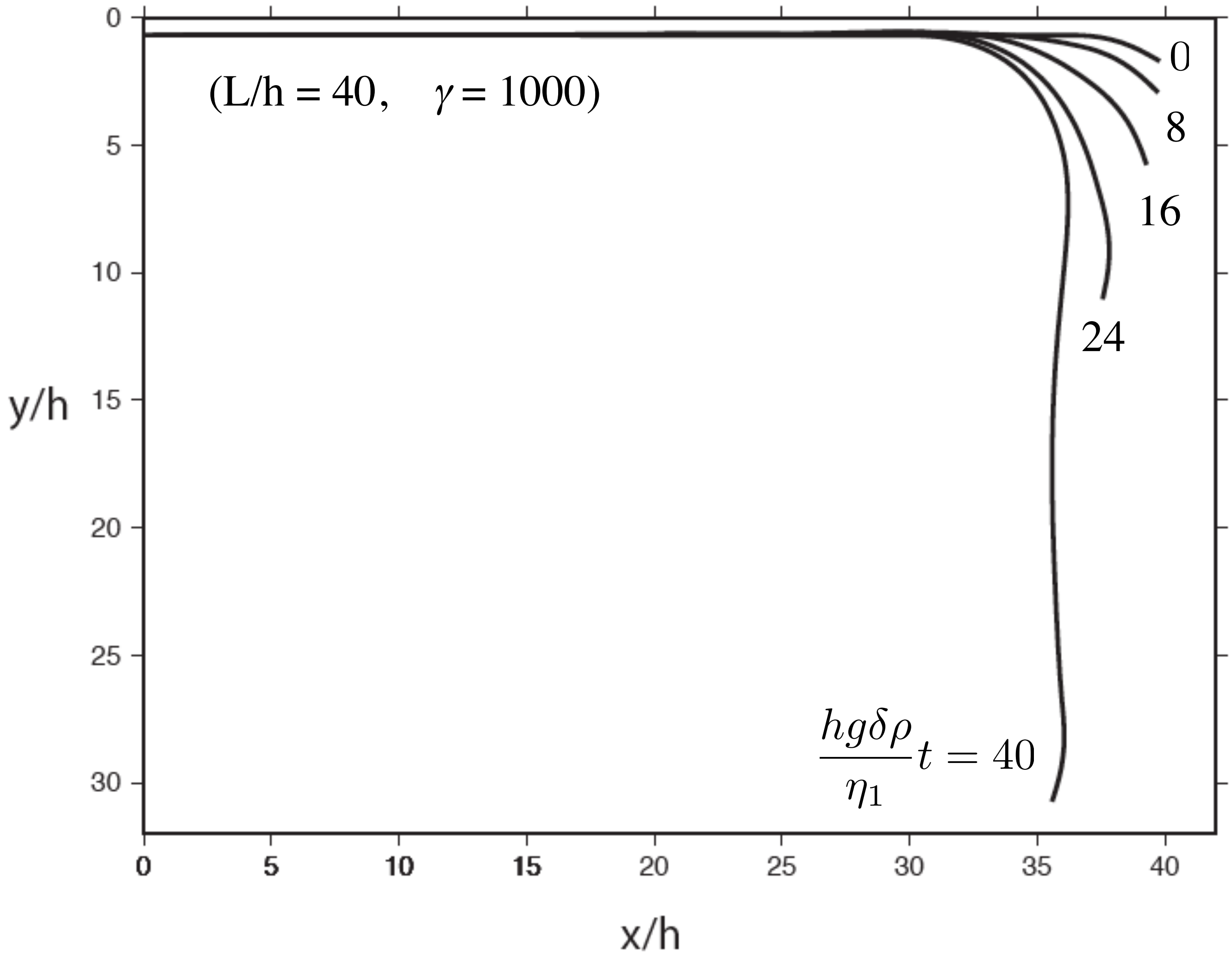

In progress: extension to nonlinear rheology → study of slab breakoff

Two-Plate Interaction at Subduction Zones

(Ph.D. thesis of Gianluca Gerardi)

Influence of the Subduction Interface on Convergence Rate

reference case
of an isolated plate
$(d_{SI} = \infty)$

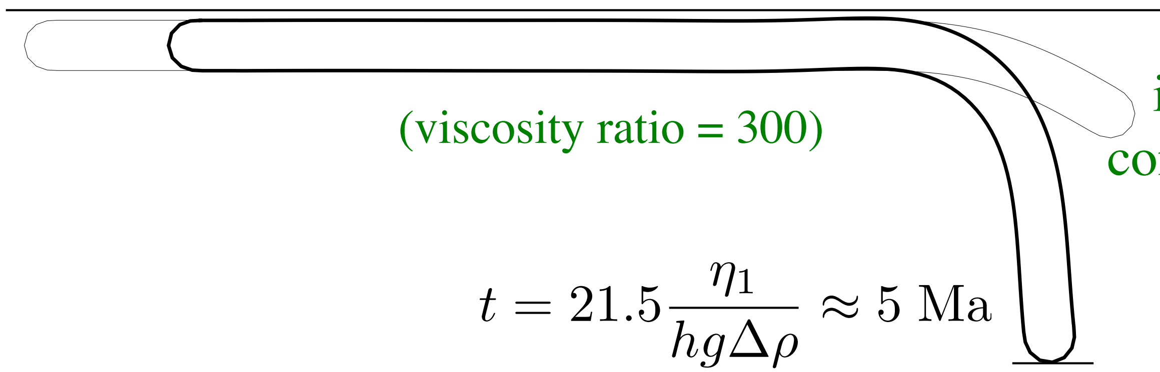

$$t = 21.5 \frac{\eta_1}{hg\Delta\rho} \approx 5 \text{ Ma}$$

$d_{SI} = 20$ km :

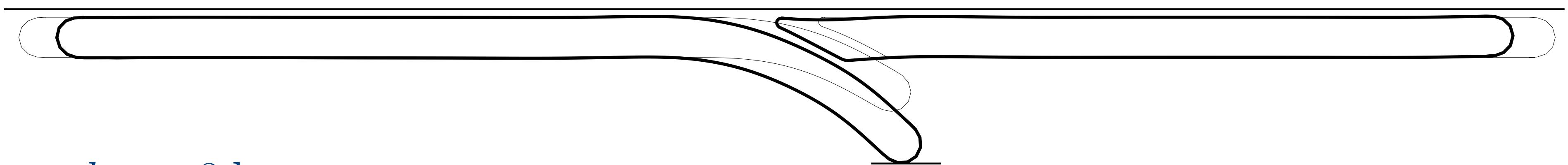

$d_{SI} = 8$ km :

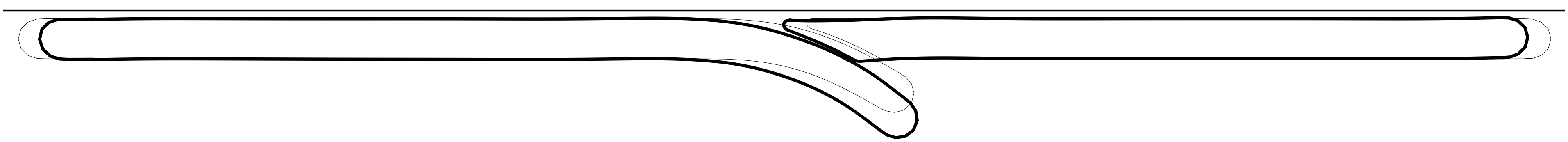

Result: convergence rate depends critically on the thickness and viscosity of the subduction interface → observed convergence rates can be used to constrain these properties

Application to the Aleutian Subduction Zone

(Lallemand et al. 2005)

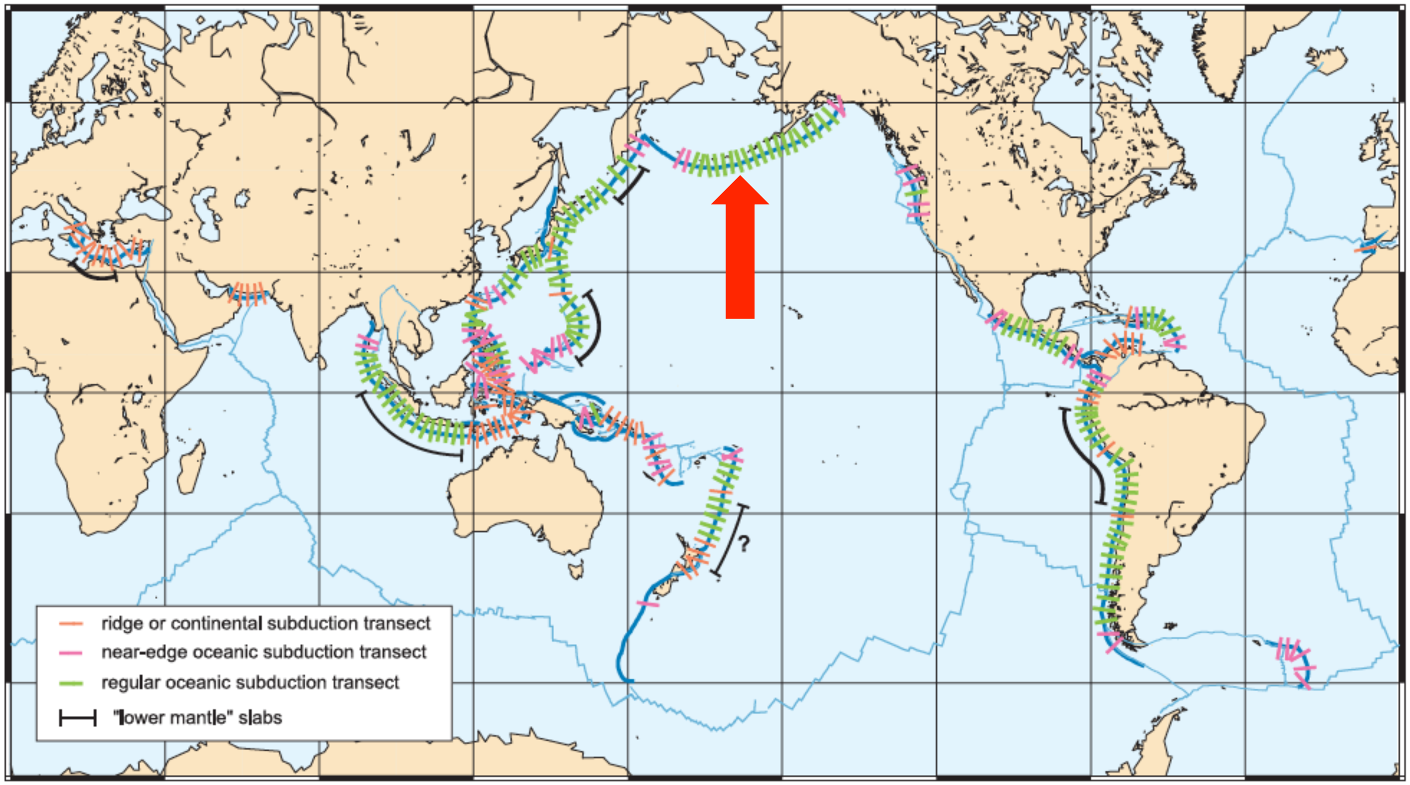

Prediction: dimensionless SI strength = $\dfrac{\eta_{SI} h}{\eta_1 d_{SI}} = 4 \pm 2$

$\rightarrow$ $\eta_{SI} = 1 - 2 \times 10^{20}$ Pa s for $d_{SI}/h = 0.07$

Dissipation Partitioning in Free Subduction

Motivation: suggestion of Conrad & Hager (1999) that the rate of dissipation in mantle convection is dominated by the plate bending contribution

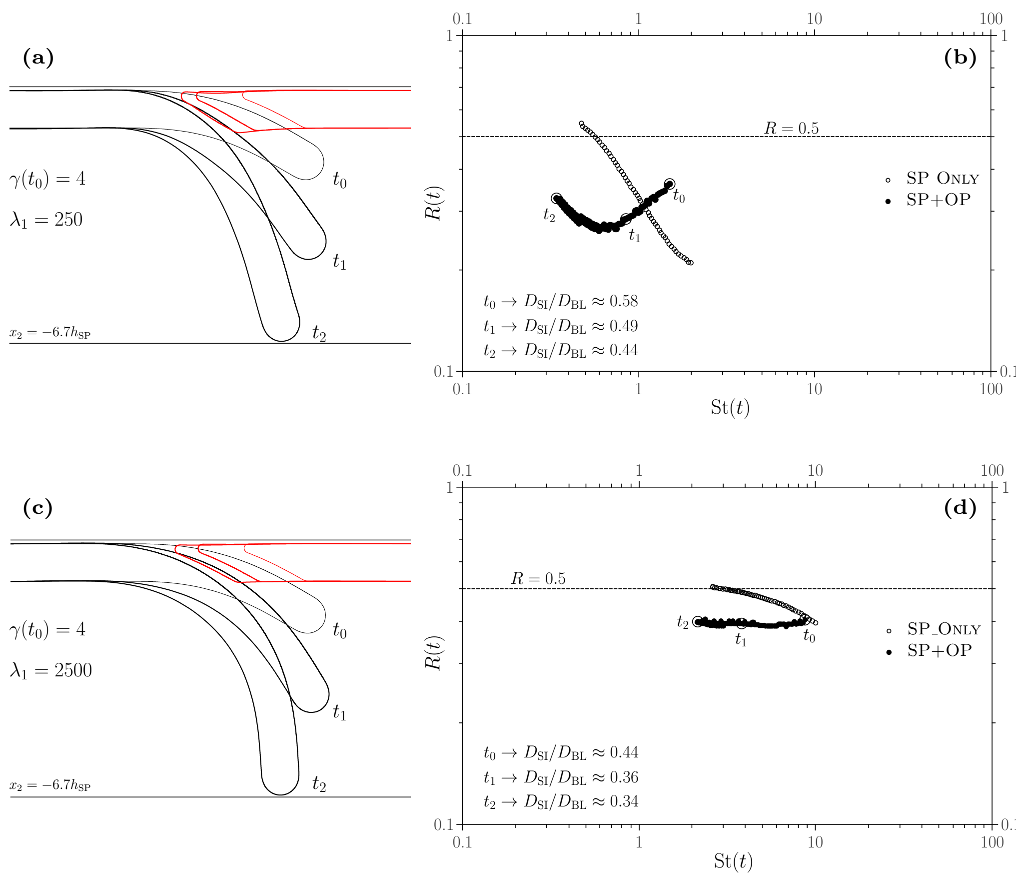

R = fraction of the total dissipation that occurs within the plates

Result: dissipation rate in the stiff upper boundary layer never exceeds 40% of the total

Conclusions

1. The fundamental length scale in free subduction is the bending length l_b (= slab length + flexural bulge)

2. The key dimensionless parameter is the flexural stiffness

$$S = \frac{\eta_2}{\eta_1}\left(\frac{h}{l_b}\right)^3$$

3. Subduction mode selection is controlled by the incidence angle of the slab on the 660 km discontinuity

4. Periodic slab folding may be occurring today beneath Central America

5. The effective viscosity of the Aleutian subduction interface is $\eta_{SI} \sim 1\text{-}2 \times 10^{20}$ Pa s

6. Viscous dissipation due to plate bending is a significant but not dominant contribution to the total dissipation rate

Slab Morphology vs. γ and H/h

Red numbers: angle at which the slab first strikes the bottom boundary

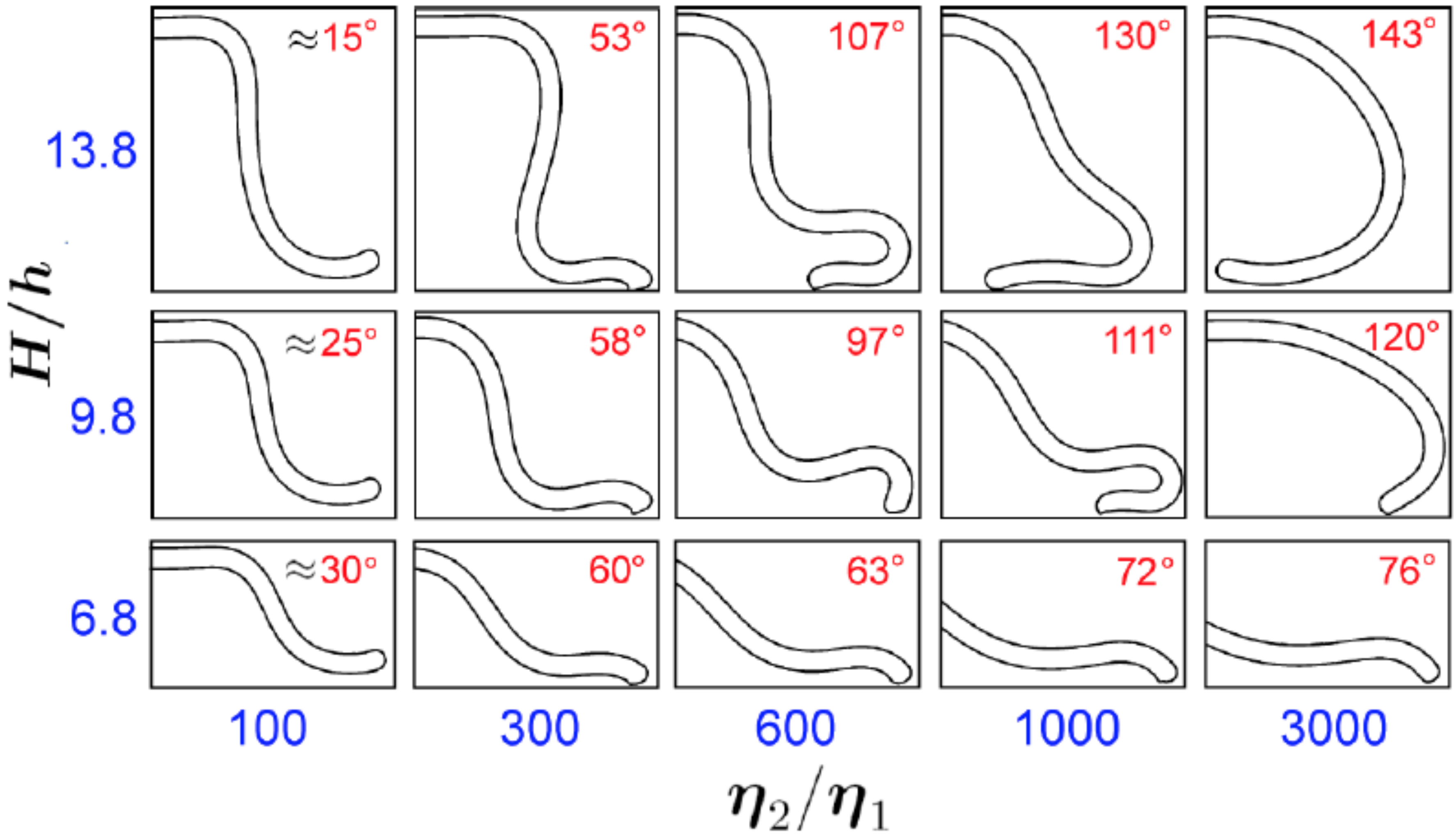

3-D Flow Pattern Around a Subducting Sheet

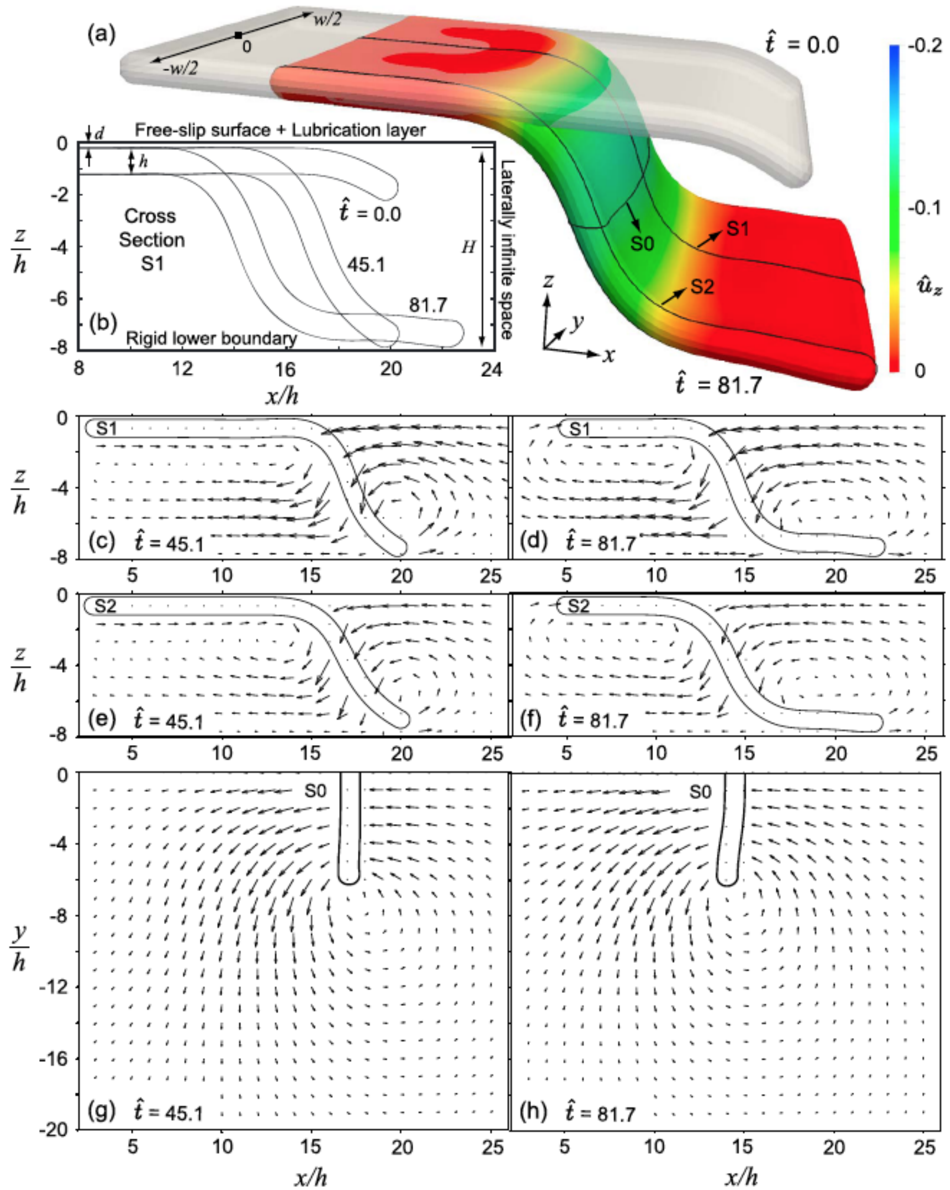

Periodic folding of subducted lithosphere?

a)

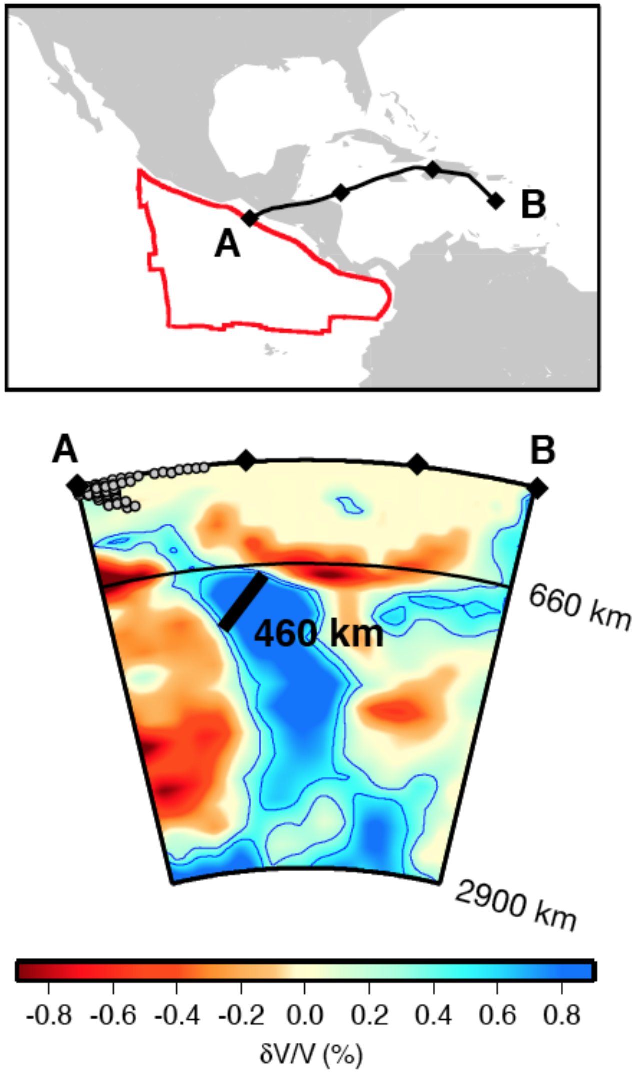

b)

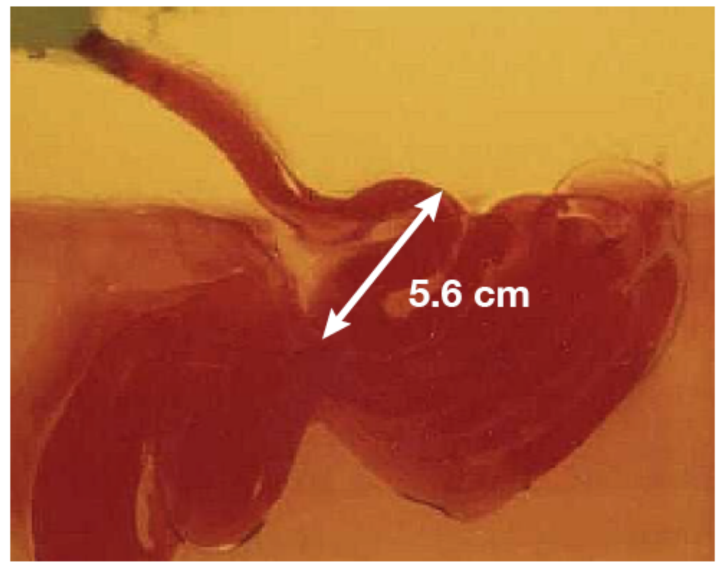

photo courtesy of P. Olson

Seismic Anisotropy at Subduction Zones

Shear-Wave Splitting at Subduction Zones

(Long & Becker 2010)

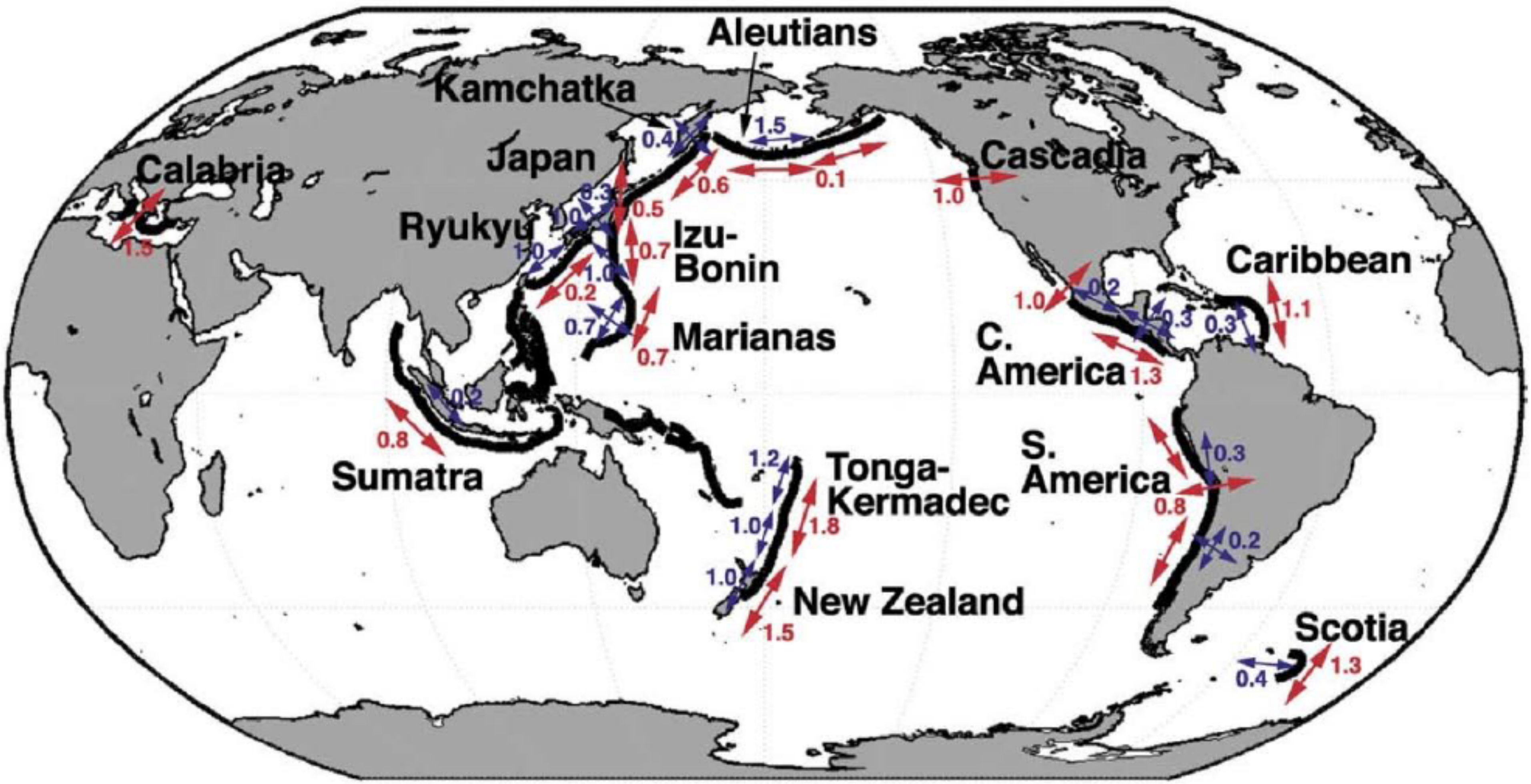

Modeling Seismic Anisotropy in Mantle Flow

(1) Simple approximate method: use finite strain as a proxy

- ☛ Seismically fast axis (a-axis) of olivine aligns with the long axis of the finite strain ellipsoid (Ribe 1992)
- ☛ Computationally trivial

(2) More rigorous method: viscoplastic self-consistent (VPSC) model

- ☛ Enforces compatibility of stresses and strain rates among grains in a polycrystal
- ☛ Computationally very intensive

3-D Reference Model for Mantle Flow

(Li et al. 2014)

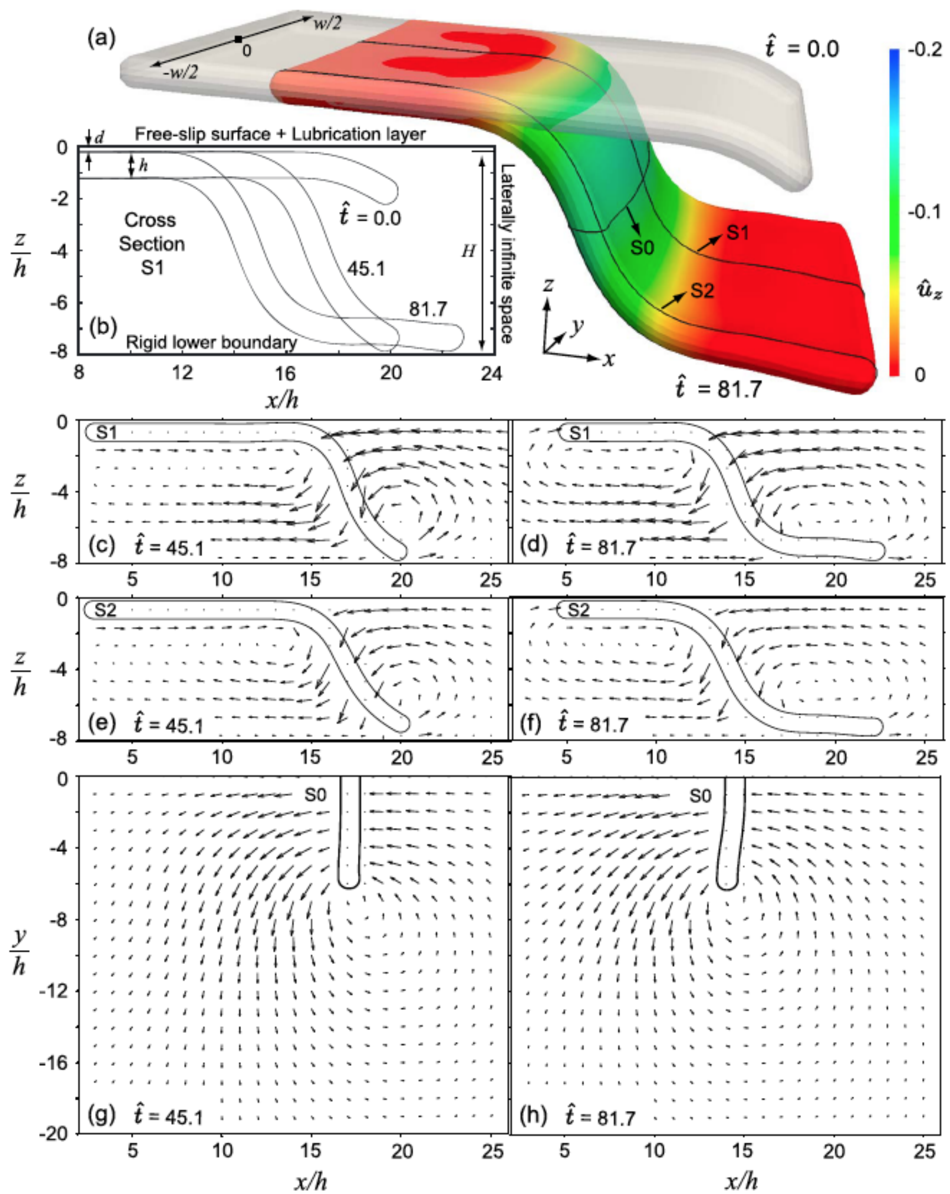

Complex Particle Paths in Subduction-Induced Mantle Flow

Calculation method:

(1) Start with a vertically aligned set of points at the end of the simulation

(2) Trace particles backward to initial time t = 0

(3) Trace particles forward again while accumulating finite strain and calculating texture using the VPSC algorithm

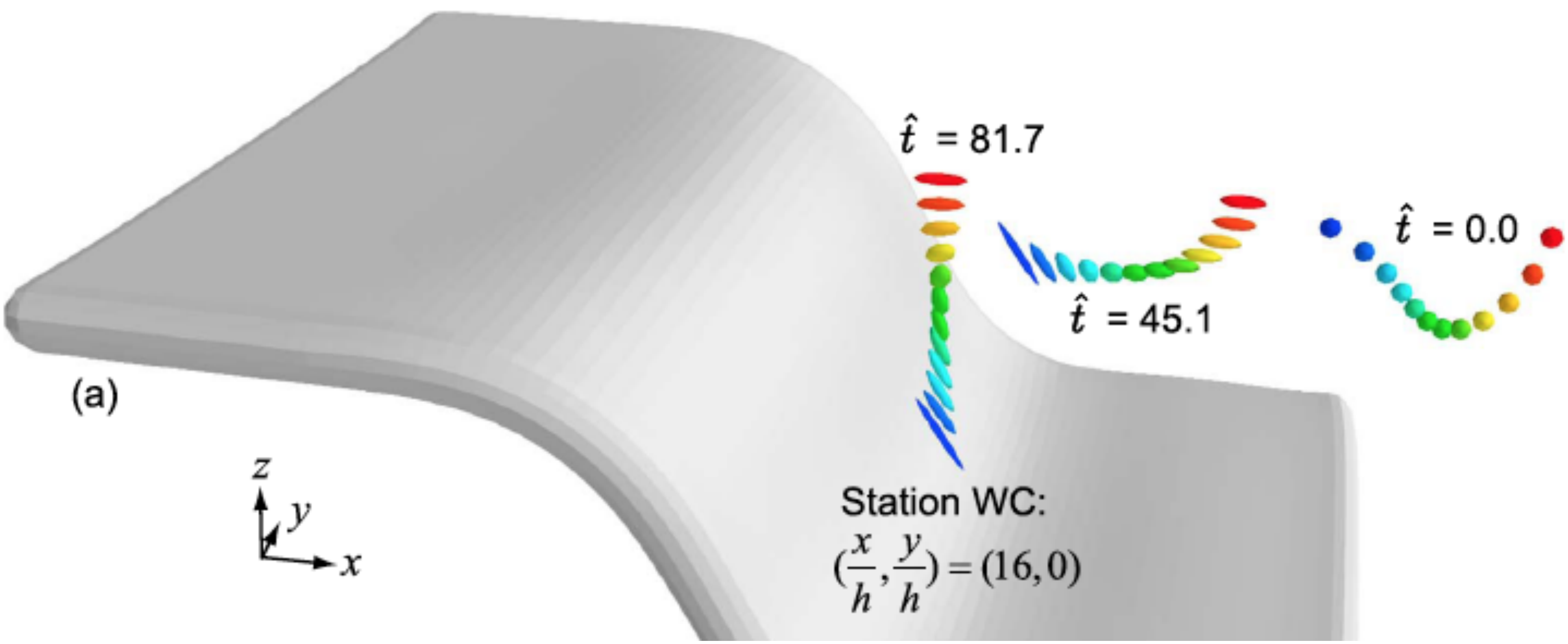

Finite Strain in the Vertical Symmetry Plane

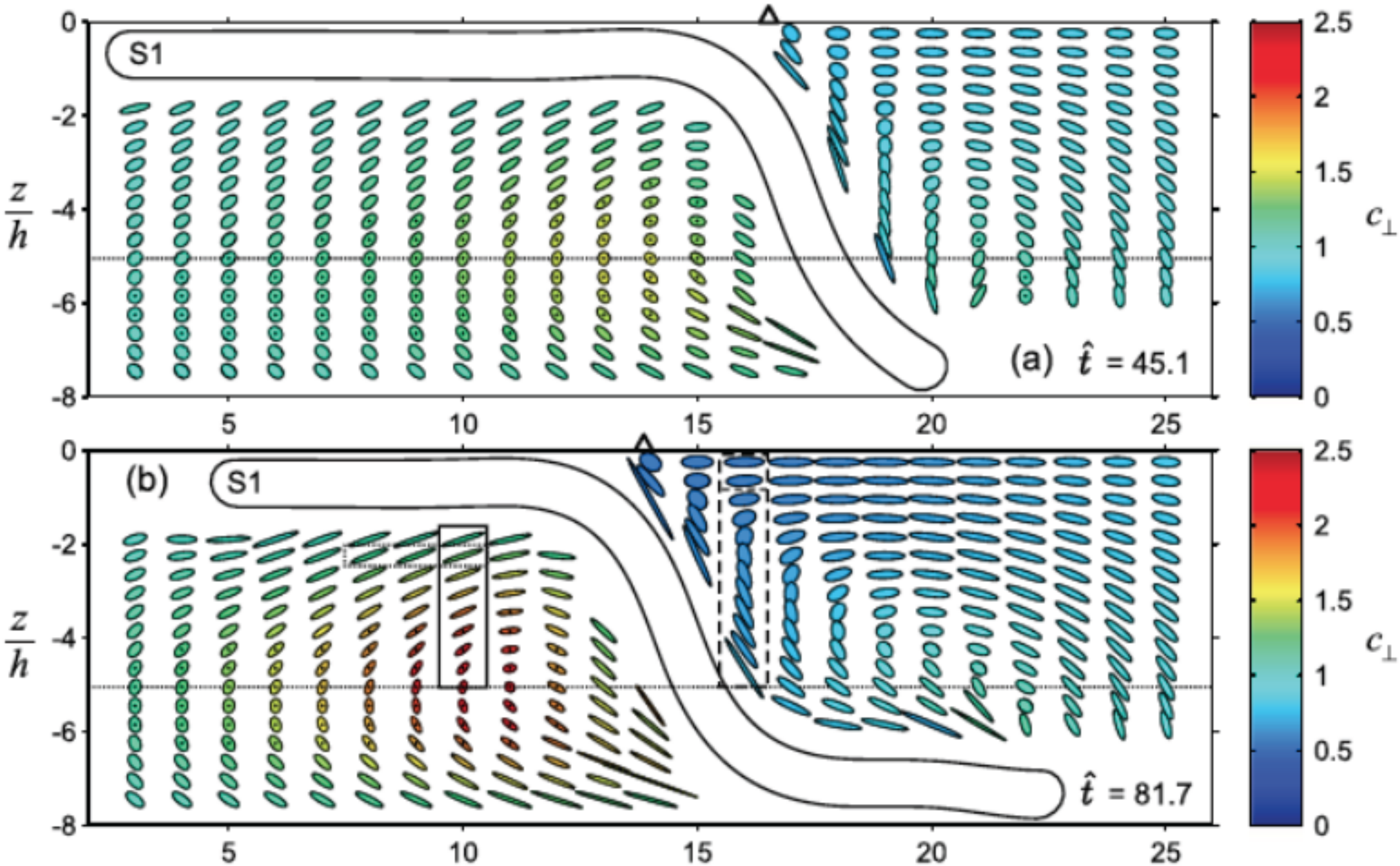

Finite Strain in the Vertical Symmetry Plane

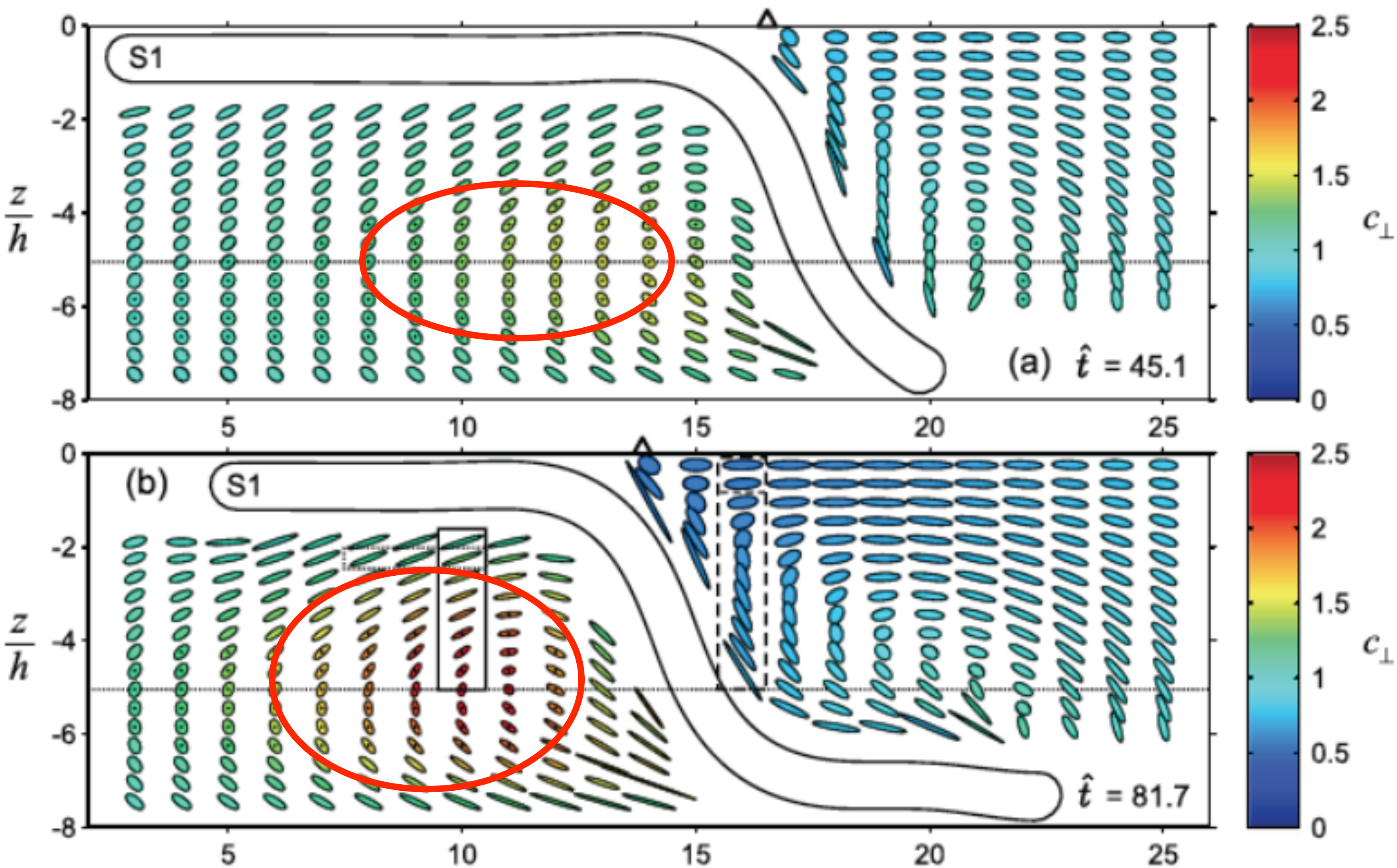

SKS Splitting: BEM/VPSC Predictions